

3-27-2013

Making Climate Data Relevant to Decision Making: The important details of Spatial and Temporal Downscaling

Evan H. Girvetz

Edwin P. Maurer
Santa Clara University, emaurer@scu.edu

Philip B. Duffy

Aaron Ruesch

Bridget Thrasher

See next page for additional authors

Follow this and additional works at: <http://scholarcommons.scu.edu/ceng>

 Part of the [Civil and Environmental Engineering Commons](#)

Recommended Citation

Girvetz, E.H., E.P. Maurer, P. Duffy, A. Ruesch, B. Thrasher, C. Zganjar, 2013, Making Climate Data Relevant to Decision Making: The important details of Spatial and Temporal Downscaling, The World Bank, March 27, 2013

Authors

Evan H. Girvetz, Edwin P. Maurer, Philip B. Duffy, Aaron Ruesch, Bridget Thrasher, and Chris Zganjar

Making Climate Data Relevant to Decision Making: The important details of Spatial and Temporal Downscaling

March 27, 2013

Dr. Evan H. Girvetz
The Nature Conservancy

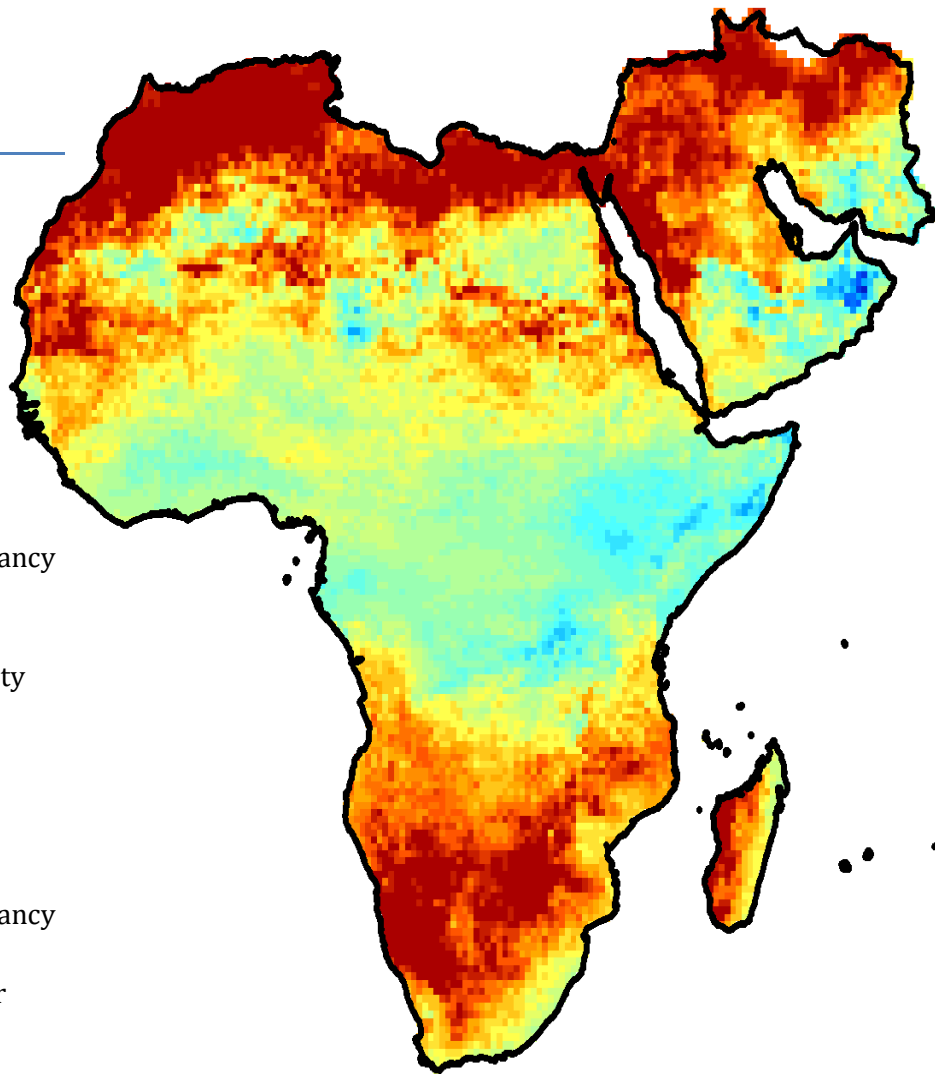
Dr. Edwin Maurer
Santa Clara University

Dr. Philip Duffy
Climate Central

Aaron Ruesch
The Nature Conservancy

Dr. Bridget Thrasher
Climate Central

Chris Zganjar
The Nature Conservancy



Contents

- Section 1: Introduction and Executive Summary 4
 - Downscaling global climate models to finer spatial and temporal scales..... 5
 - Translating climate models into specific impacts 7
 - Data dissemination, analysis, and decision support tools 8
- Section 2: Downscaling climate models to a daily time scale..... 9
 - Different types of downscaling approaches 9
 - Dynamical Downscaling..... 9
 - Statistical downscaling 9
 - Daily bias-corrected spatial disaggregation (BCSD) downscaling 10
 - Daily downscaling method..... 11
 - Bias-correction..... 13
 - Trend Preservation 13
 - Quality Control of daily downscaled climate models..... 14
- Section 3: Calculating derivative climate metrics 16
 - Methods for calculating derivative metrics 16
 - Derivative Climate Metric Applications..... 20
 - Quality Control of Derivative Statistics 21
- Section 4: Climate change analysis and visualization..... 23
 - Selection of Time period 23
 - Aggregated versus grid-based analysis 23
 - Different Types of Climate Change Analyses..... 24
 - Summary of different types of climate analyses 24
 - Average climate 25
 - Departure change analysis..... 26
 - P-value: statistical confidence in change 27
 - Future recurrence interval..... 28
 - Ensemble Analysis..... 30
 - Quantile ensembles 30
 - Climate model-weighted ensembles..... 30
 - 31

Looking at regional patterns versus single climate grid cell	31
Section 5: Using daily downscaled data in impact modeling.....	33
Cited References	38
Appendix 1: Quality control for daily downscaled climate models	40
Appendix 2: Derivative statistics data ranges for summarized across all climate models.....	43

Section 1: Introduction and Executive Summary

Throughout the world, there is a major need for climate change science to inform on-the-ground adaptation planning. However, a major gap exists between the well-developed state of climate science and decision-makers preparing for a future climate. There is no shortage of scientific data that has been produced about climate change, but very little of this information is relevant to on-the-ground decision making about these types of specific climate change impacts. This is due to different reasons: 1) the climate model information is at spatial and temporal scales too coarse a scale for most impact modeling (200-500 km and monthly averages) that often do not well represent local climate impacts; 2) General Circulation Models (GCMs, also known as global climate models) outputs focus mostly on changes to temperature and precipitation rather than specific impacts relevant to people; and 3) almost all of the climate change information available is stored in difficult to access formats (e.g. NetCDF Files).

Climate models projecting future conditions need to better translated into packets of information useful for decision-makers. There is a wide variety of information needed depending on the type of issue being addressed and the level of technical ability at hand. Users of climate information will range from highly technical scientists and engineers running climate impact models to non-technically trained local community members planning adaptation responses. However, there are similarities in what is need for virtually any decision-making situation: future climate information at the spatial and temporal scales relevant to specific climate impacts in local places throughout the world. People need to know more than just about changes to temperature and precipitation at a global scale, they need this information translated into impacts to agriculture, water supply, fire risk, human health, urban energy demand, and among others for specific places on-the-ground.

Translating climate models to provide decision-support requires three main things for linking climate science to decision makers (Figure 1): 1) downscaling global climate models to finer spatial and temporal scales; 2) translating changes to temperature and precipitation into specific impacts to agriculture, hydrology, health, ecosystems, and urban energy demand, among others; 3) presentation and dissemination of these data to specific users throughout the world.

The focus of this document is n how these three issues are being addressed to bring relevant climate information to adaptation and risk planning globally.

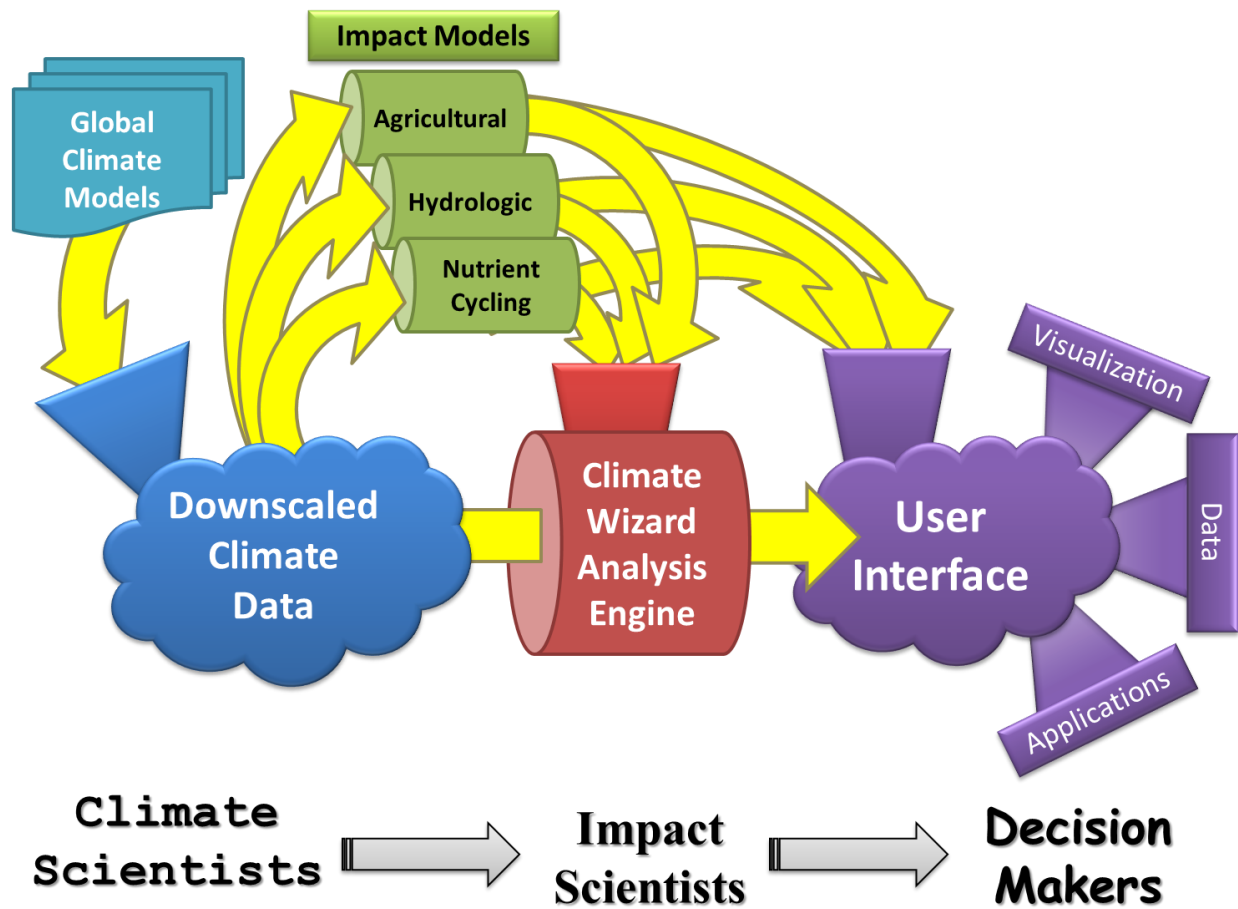


Figure 1: Climate data analysis and web-based visualization framework that links together: 1) downscaled climate projections developed by climate scientists; 2) the Climate Wizard analysis engine to query and analyze climate databases for geographic places; 3) impact models that translate climate into specific impacts in specific locations; 4) user interfaces that link users to the climate data through web-based mapping applications.

Downscaling global climate models to finer spatial and temporal scales

Global climate model information can be enhanced to better represent the conditions we know have occurred in specific places by using historically observed local climate information from weather stations. First, this local information allows for the future climate models to be downscaled from 200-500km (40,000 – 250,000 km²) to much finer scales to overcome the problem of these models being too coarse. Second, this information can be used to modify the future climate projections to better match observed local climate conditions—a process known as “bias-correction”. Downscaling and bias-correcting at both a finer spatial and temporal resolution is needed to better represent the influence of topography and regional climate patterns on both the average and variation in climate, and to more accurately and completely assess future climate impacts.

Spatially downscaling and bias-correcting climate models is commonly conducted, however this is generally only done at monthly and annual time scales (e.g., Maurer et al. 2009; <http://ClimateWizard.org>). Downscaling and bias-correcting at a daily time scale is important for assessing climate impacts for a few reasons. First, it is generally not the average monthly condition

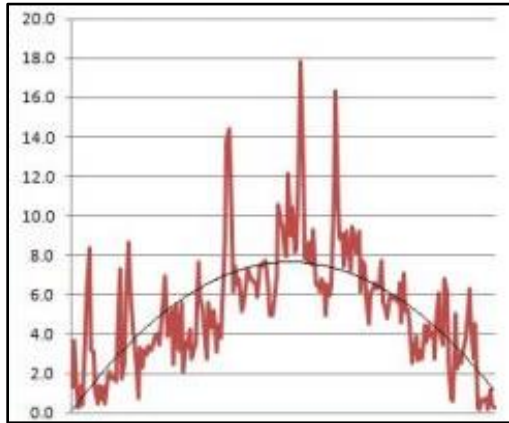


Figure 2: Example of the monthly average climate during a calendar year (black line) compared to day-to-day variation showing peaks and valleys (extreme hot and cold days or wet and dry days during a single calendar year).

that causes impacts, but rather the extreme peaks and valleys in the climate throughout the year and over decadal time-scales (Figure 2), or the extreme tail of climate events (i.e., infrequent events with severe impacts, Figure 3). Second, many climate driven impacts occur as a cumulative effect of what happens at the daily time scale—for example growing degree days are often used to determine agricultural suitability—and cannot be accurately estimated from monthly data. Third, most hydrologic, agricultural, and other impact models commonly require daily climate data in order to produce results relevant to real-world decision-making.

A collaborative effort between The World Bank, The Nature Conservancy, Climate Central, and Santa Clara University has now produced the first standardized set of daily downscaled GCM projections that span the entire globe (See Section 2). This includes all terrestrial

daily data archived in CMIP3 (http://www-pcmdi.llnl.gov/ipcc/about_ipcc.php)—the standard for raw GCM data distribution from the IPCC Fourth Assessment Report: nine different GCMs, some with multiple model runs, across three different greenhouse gas emissions scenarios (SRES A2, A1b, B1), totaling 53 future projections, all downscaled to a 0.5 degree resolution (~50 km) for the time periods of 1961-1999, 2046-2045, and 2071-2100. These data were downscaled using bias correction-spatial disaggregation (BCSD) methods adapted to a daily time scale from previous BCSD downscaling applied at a monthly time scale (Maurer et al. 2007). As part of downscaling it is important to bias-correct the climate model data to best represent the historic observation measured in the real world.

Such a data set has yet to be developed for various reasons. For one, on the CMIP3 archive, most are available only at a monthly or annual time scale, although a sub-set of GCMs are achieved at a daily time scale. Second, downscaling methods have traditionally been developed for monthly data, and so monthly downscaled data are the default. Third, there have been computational power and storage space limitations to developing downscaled daily data.

The daily downscaled outputs total 3.5 Terabytes. The availability of these data now to the scientific and practitioner communities around the world, represent a large step in bridging the gap between climate science and on-the-ground decision making.

This data set forms the basis for developing climate change analysis metrics and analyses useful for supporting adaptation decision making and modeling climate change impacts that are summarized below and presented in sections 3-5.

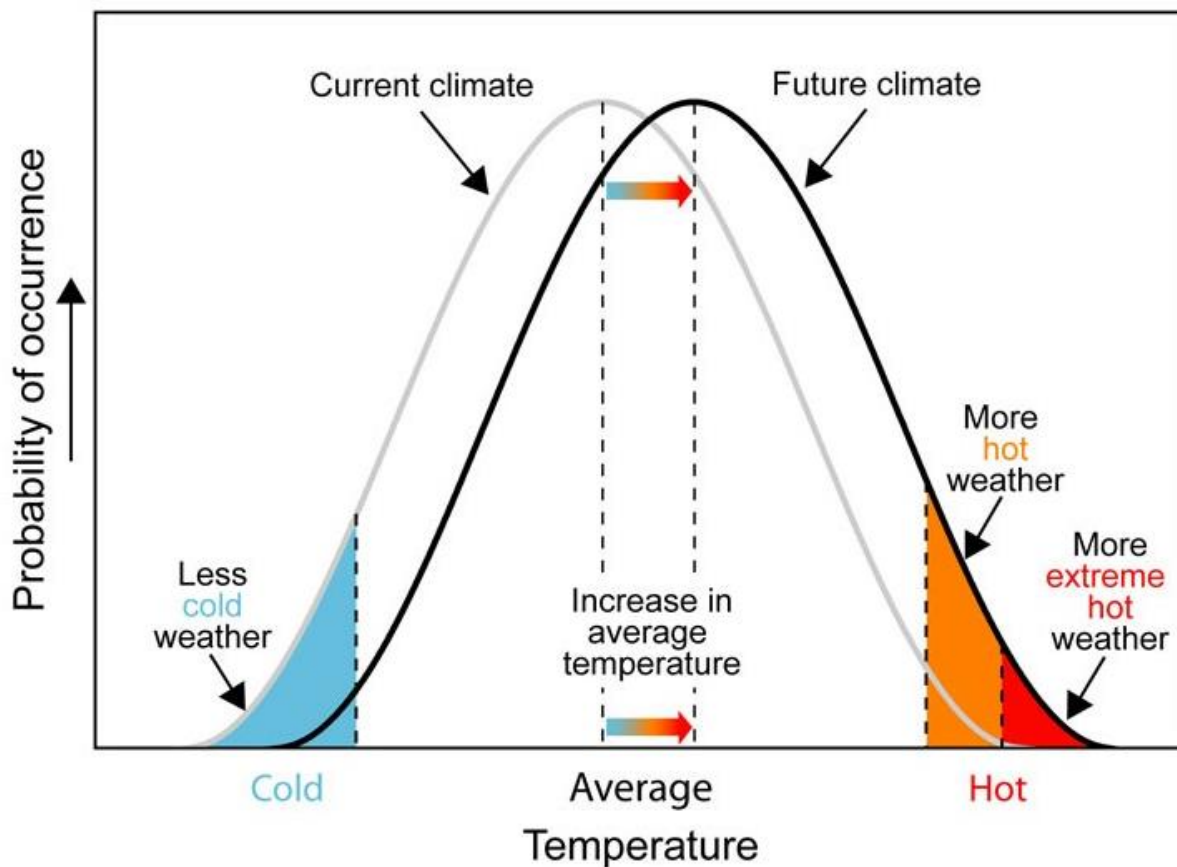


Figure 3: Hypothetical distributions of previous and new (future) climates showing change in the average temperature and how that translates to changes to extreme events (from <http://SouthwestClimateChange.org>, modified from IPCC 2007). Note that the extreme hot events shown in orange and red become disproportionately more likely to occur in the future than in the past, whereas extreme cold events become disproportionately less likely to occur.

Translating climate models into specific impacts

Knowing how temperature and precipitation is projected to change in the future on average is not very useful to decision-makers planning for specific types of impacts to agriculture, water supply, fire risk, human health, urban energy demand, biodiversity, among many others. Rather, temperature and precipitation need to be used to create more useful climate metrics and impact modeling results that can be used directly to inform the development of climate adaptation responses. This can be done in at least a couple of ways: 1) calculating derivative climate metrics based on daily downscaled future climate projections that represent surrogates of different types of climate impacts; 2) running sector specific climate impacts models—such as crop yield models and river flow hydrologic models—that are driven by daily downscaled future climate projections.

First, a set of 22 “derivative climate metrics” that have been calculated from the daily downscaled climate are presented in Sections 3 and 4. These metrics include growing degree days, the hottest day of each year, and most amount of rain that falls in a 5-day period each year (See appendix 1 for complete list). Applications of these climate metrics and how they can be used to support climate preparedness planning are also discussed.

Second, agricultural, hydrologic, among other impact models often require daily climate data, and the lack of readily available daily future climate projections has been a barrier to doing climate change impact assessments for specific places throughout the world. These daily downscaled data now provide a means for using these types to assess future climate change impacts. See Section 5 for a discussion of integrating these data into impact modeling and case-study examples of how these data can be used for running agricultural and hydrological models.

Data dissemination, analysis, and decision support tools

It is not enough to simply develop climate data—in addition, there is a need to deliver these data to decision-makers, planners, engineers, and scientists in useful formats. This includes summaries of climate change information in the form of maps, graphs and tables for specific areas of interest throughout the world. Building on the foundation of tools currently available—including the World Bank Climate Knowledge Portal (<http://sdwebx.worldbank.org/climateportal/index.cfm>) and Climate Wizard (<http://ClimateWizard.org>), Section 4 here presents how the derivative climate metrics presented here are being served to users through a website application.

Section 2: Downscaling climate models to a daily time scale

Different types of downscaling approaches

There are two commonly used methods downscale future climate projections to finer spatial scales: *dynamical downscaling* (also referred to as “Regional Climate Models”) and *statistical downscaling* (sometimes called “empirical”).

Dynamical Downscaling

Dynamical downscaling generally uses a nested modeling approach where a regional climate model is run for a restricted area of the globe with boundary conditions forced by a global climate model. This method has the advantage that it is based on physical laws and can, in theory, better represent localized feedbacks in response to increased greenhouse gas concentrations and global warming. This downscaling method can produce a full suite of different output variables from the downscaling process because it is based on physical laws rather than statistical properties of historic climate. However, it is computationally very demanding, making it infeasible to run on a global scale or for many different climate models. In addition, since the dynamical downscaling is connected to global climate models, errors from those models will be propagated through the downscaling—“garbage-in garbage-out”.

<u>Nested Dynamical Downscaling</u>	
Advantages	Disadvantages
<ul style="list-style-type: none">• Based on physical laws, so should correctly represent local feedbacks in response to increasing GHG.• Produces a full suite of output variables.	<ul style="list-style-type: none">• Computationally very demanding• Generally preserves biases (errors) from the driving GCM—“garbage-in, garbage-out”• Most GCM simulations don’t save output needed for dynamical downscaling• Difficult to downscale a large number of future climate projections

Statistical downscaling

Statistical downscaling (also called empirical downscaling) is a commonly used method for downscaling because of the relative ease of application and the flexibility of the method for different applications. Because of their wide use, statistical downscaling methods have been well tested and validated in many environments. The principal disadvantage of statistical downscaling is its assumption that the derived statistical relationships between coarse-scale climate simulated by GCMs for historical periods and the fine-scale climate features observed in the past will be the same

in the future. Even with the natural variability of this relationship, this assumption has been found to be reasonable on average (for example, Maraun, 2012; Wood et al, 2004).

<u>Statistical/Empirical Downscaling</u>	
Advantages	Disadvantages
<ul style="list-style-type: none"> • Computationally not very demanding • Does not require special output from the GCM • Can be applied to large ensembles of GCM simulations, allowing quantification of consensus. • Can include correction of GCM biases (errors) of GCM biases 	<ul style="list-style-type: none"> • Produces results for only a few variables (usually Temperature and Precipitation) • Accuracy limited by availability of gridded observations (garbage-in-garbage-out) • Relationships derived from observations assumed to apply in the future, this is not true where local feedbacks important • Bias correction derived in historical period is assumed to apply in the future.

Daily bias-corrected spatial disaggregation (BCSD) downscaling

The daily timescale Bias-corrected Spatial Disaggregation (BCSD) downscaling method was selected for this dataset because it feasibly can downscale of multiple global climate models (GCMs) on a global domain. Dynamical downscaling methods can do this in principle but in practice are hampered by computational limitations. Other statistical/empirical downscaling methods that work on a daily scale (e.g. bias-corrected constructed analogues method; Maurer and Hidalgo, 2008) cannot be applied meaningfully on a large scale, and certainly not on a global domain due to both data requirements and computational limitations. BCSD has been applied over regional and continental domains in many different climates (for example, the Northeastern U.S., Hayhoe et al, 2008; the Western U.S., Barnett et al.; 2008 Latin America Maurer et al., 2009; Africa, Beyene et al., 2010). The BCSD method has also been applied to examine climate change impacts on diverse sectors including agriculture, hydropower and energy, water resources, wildfire, air quality and public health, and ecosystem responses (see for example Hayhoe et al, 2004, Cayan et al 2008 and references therein). The wide applicability of BCSD across different spatial and temporal scales and use in different impacts studies makes it unique among statistical downscaling methods, and appropriate for the current effort.

Note that for the historical period the downscaled GCM output will statistically match the observations by construct. The sequencing of years, however, will not correspond to observations, since GCMs are not constrained to reproduce the timing of natural climate variations, such as El

Niño-southern Oscillation. That is, on average the mean and variance of climate from the GCMs and observations for the historic baseline period will closely match, but any given year (e.g. 1979) will not necessarily match between the GCMs and the observations.

<u>Bias-corrected Spatial Disaggregation (BCSD) Downscaling</u>	
Advantages	Disadvantages
<ul style="list-style-type: none"> • Produces results on a uniform spatial grid • Preserves long-term trends from the GCM • Allows GCM to simulate changes in variability • Can produce monthly or daily results 	<ul style="list-style-type: none"> • Results for projected temperature <i>changes</i> have no fine detail, due to a consequence of preserving trends from the GCM

Daily downscaling method

Daily precipitation, minimum temperature and maximum temperature were downscaled using the BCSD method for 53 future climate projections from the World Climate Research Programme's (WCRP's) Coupled Model Intercomparison Project phase 3 (CMIP3) multi-model dataset. The projections were from 9 global climate models (GCMs) run under three greenhouse gas emissions scenarios (some GCMs had multiple model runs), which represents all daily GCM data available from the CMIP3 archives (see Table 1 for list a GCMs downscaled). GCMs with daily archived data were obtained from the CMIP3 archives, cleaned and checked for quality, completeness and consistency. While quality checking the data from the CMIP3 archives, the BCCR_BCM2_0 A2 and B1 model run was found to be corrupt and unfixable, and thus was omitted from the list of models downscaled.

Downscaled results were produced on a global domain (land areas only), with daily time resolution on a spatial grid of 0.5° in latitude by 0.5° in longitude. Because of limited availability of daily-timescale GCM output, downscaled results were produced for three limited time windows: 1961-1999 (referred to below as the historical reference period), 2046-2065, and 2081-2100.

Table 1: The following list of GCMs, scenarios and model runs were obtained from the CMIP3 archives for the time periods 1961-1999, 2046-4065, and 2081-2100.

GCM Code	Formal Name	Scenario (# of runs)			Native Model Resolution (°lat x °lon)
		B1	A1B	A2	
cccma_cgcm3_1	CGCM3.1 (T47)	3	3	3	3.75 x 3.75
cnrm_cm3	CNRM-CM3	1	1	1	2.8125 x 2.8125
gfdl_cm2_0	GFDL-CM2.0	1	1	1	2.0 x 2.5
gfdl_cm2_1	GFDL-CM2.1	1	1	1	2.0 x 2.5
ipsl_cm4	IPSL-CM4	1	1	1	2.5 x 3.75
miroc3_2_medres	MIROC3.2 (medres)	2	2	2	2.8125 x 2.8125
miub_echo_g	ECHO-G	3	3	3	3.75 x 3.75
mpi_echam5	ECHAM5/ MPI-OM	1	0	1	1.875 x 1.875
mri_cgcm2_3_2a	MRI-CGCM2.3.2	5	5	5	2.8125 x 2.8125
Total		18	17	18	

The downscaling method used was a daily-timescale variant of a method known as Bias Correction/Spatial Downscaling (BCSD) that has been widely applied to produce monthly downscaled quantities based upon monthly GCM results. The monthly version of the method is described by Wood et al. (2002 and 2004). Further documentation can be found online at http://gdo--dcp.ucllnl.org/-downscaled_cmip3-projections/-dcpInterface.html. As with any statistical downscaling method, some assumption of stationarity is needed. For the technique used in this study it is assumed that the processes shaping the climate at the fine grid scale during the historical period will continue to govern local climate features in the future, which may not always be the case. Past work has shown that the statistical BCSD method as implemented here performs comparably to dynamical downscaling approaches, at least when assessing hydrologic impacts of climate change.

A daily variant, which produced daily timescale downscaled results based upon daily timescale GCM results, is described by Abatzoglou and Brown (2011). This daily downscaling is not to be confused with temporal disaggregation, which produces daily values based upon monthly GCM results and some questionable assumptions. Here we used a daily variant of the BCSD that is similar to that of Abatzoglou and Brown (2011), but which was developed independently.

The downscaling and bias-correction was done using historical *observed daily* gridded observations. The base meteorological data consists of daily time-series for the period of 1950 through 1999 of precipitation, maximum temperature and minimum temperature. Monthly station data from a variety of sources (including the Global Historical Climatology Network (GHCN) version 2 data) were compiled and gridded to a resolution of 0.5-degree over all global land areas. The daily variability of precipitation, maximum and minimum temperature was constructed using other global daily datasets, which were scaled to match the monthly values. See Table 2 below for more information and complete methods used.

Table 2: Data sources to create the 1/2-degree gridded global meteorological data for 1950 through 1999 (based on Maurer et al 2009).

Description	Reference	Variable	Time Step	Period of Use	Application
University of Delaware Climate Data	Willmott and Matsuura (2001)	Precip	Monthly Time Series	1950-1999	To create monthly precipitation variability
East Anglia Climatic Research Unit Climate Data	New et al. (2000) and Mitchell et al. (2004)	Tmax Tmin	Monthly Time Series	1950-1999	To create monthly precipitation variability
University of Washington Gauge Catch Corrections	Adam and Lettenmaier (2003)	Precip	Monthly Climatology	1950-1999	To apply the montly precipitation time series to correct for systematic bias
Princeton University corrections to NCEP/NCAR reanalysis	Sheffield et al. (2006)	Precip Tmax Tmin	Daily Time Series	1950-1995	To create daily variability by rescaling these data to match the monthly variability of the above time series
University of Washington stochastically-generated climate data	Nijssen et al. (2001)	Precip Tmax Tmin	Daily Time Series	1996-1999	To create daily variability by rescaling these data to match the monthly variability of the above time series

Bias-correction

The bias correction step is performed independently for each day of the year (January 1 through December 31). For each day, we based the bias correction on results from the reference period within +/- 15 days of the day in question. For example, for February 20 (the 51st day of the year), the bias correction is based upon results from days $51 - 15 = 36$ through $51 + 15 = 66$, for all 40 years in the reference period (i.e. a total of 40×31 days). That is, the bias correction for February 20 is determined by comparing reference period results from days 36 through 66 in the GCM to results from the same set of days in observations. Using these data, the bias correction process itself is the same quantile mapping approach described in the references cited above.

Trend Preservation

A potential hazard of the bias correction process is that it cannot distinguish between year-to-year variability and an underlying trend (such as from increasing greenhouse gases)—these both create an increased range of values. Thus, bias correction of data with an underlying trend would tend to artificially adjust variability downwards. This would not only produce incorrect interannual variability in the bias-corrected results, but also tend to remove the underlying trend. To avoid these tendencies, we remove any underlying trend from the results before bias correction, and add it in again afterwards. This ensures that the bias correction adjusts the interannual variability

properly, and that trends in the bias corrected results are the same as before bias correction. Because the downscaling step does not alter trends, either, this implies that trends in our BCSD results are the same as in the original GCM results. This realizes an important principle, namely that the GCM is the best source of information about long-term trends; hence bias correction and downscaling should preserve those trends.

The trend-determination process we used is influenced by the fact, noted above, that daily GCM data is unavailable for the periods 2001-2045 and 2066-2080. Hence any process that determines a trend in the 21st century results has to be robust to the reality that the first 44 years of data are missing.

The trend preservation process involves the following steps:

- a. Calculate monthly means for all data;
- b. Calculate monthly climatologies for 1961-1999; i.e. the mean of all Januaries, the mean of all Februaries, etc;
- c. Calculate monthly anomalies relative to the climatologies described above;
- d. Calculate the 9-year running mean of anomalies for each month (this is the "trend");
- e. Set the trend to zero during 1961-1999;
- f. Subtract the trend from each day in the month in question;
- g. Perform bias correction on detrended results;
- h. Add trend removed in step (f) to the detrended results.

All climate models listed in Table 1 were downscaled to a 0.5 degree resolution and daily time scale for the years 1961-1999, 2046-2065 and 2081-2100.

Quality Control of daily downscaled climate models

Any complex calculation of the type described here is vulnerable to errors. These can originate from defective input data, poor choice of algorithm, or imperfect implementation of chosen algorithm. The volume of data involved prohibits "hand-checking" of all but a few representative results. To minimize the possibility of errors, therefore, we designed and implemented a quality control process that checks key aspects of the results. Of course, any process of this type only minimizes the likelihood of errors, and cannot guarantee error-free results.

We summarize quality-checking steps that were performed on the daily downscaled climate products, for each of the general circulation models. All results were found to be within expected tolerances. See Appendix 1 for complete results from the quality control analysis.

For daily minimum and maximum temperatures, the following were checked:

1. The maximum value of Tmax and the minimum value of Tmin for both the 20th and 21st century periods (see table below for minimum and maximum values for both Tmin and Tmax).
2. The number of cases where $T_{min} < -50$ C, and $T_{max} > 50$ C

3. Compared at each location the median values of bias-corrected (but not downscaled) model results to those in observations. By design, the median value for the bias-corrected data (for the 30-day moving window) should precisely agree with the 30-day moving window median value of the observed data.
4. Compared at each location the overall trend before vs. after bias correction. The bias correction procedure is designed to preserve trends.

For precipitation results, the following were checked:

1. Negative values of precipitation.
2. Daily precipitation values in excess of 400 mm/day. Such values are not necessarily erroneous, but they should not occur too often. We calculated the rate of occurrence of such values in the 20th and 21st centuries.
3. Locations where precipitation occurs every day.

Section 3: Calculating derivative climate metrics

Interpreting changes to daily climate change is challenging without running the type of sophisticated climate impact models described in Section 5. However, a variety of “derivative climate metrics” can be calculated from daily future climate projections that to provide insight and interpretation without running technical models. These derivative climate metrics allow for a more easy and intuitive way to interpret changes to daily climate data which can be interpreted as surrogates for impacts agriculture, water supply, flood risk, human health, energy demand and ecosystem resilience. These include metrics such as growing degree days (agriculture), the hottest day of any given year (human health), and the most amount of rain that falls in a five-day period each year (flood risk). Using the daily downscaled future climate projections described in Section 2 above, 22 derivative statistics are described in this section and are available as part of the World Bank Climate Portal powered by Climate Wizard (described in Section 4).

Methods for calculating derivative metrics

To be consistent with past efforts calculating similar extreme climate statistics, we used the source code developed and distributed by the Max Plank Institute (MPI) for Meteorology. The code is a set of commands wrapped into a package called the Climate Data Operators, Version 1.5.0 (March 2011). All source code can be obtained at the MPI site <https://code.zmaw.de/projects/cdo/files>.

We calculated a suite of 22 statistics using daily downscaled GCM output, with most of these statistics being widely used for many years in the climate community for characterizing extreme events (e.g., Easterling et al., 2003; Karl et al., 1999). Typical values, for historic periods, of many statistics are illustrated by Fritch et al (2002).

In the tables above, the calculation of each statistic is described, and some more complete descriptions are in the literature (e.g., Schulzweida et al., 2011, von Engelen et al., 2008). Many of these statistics have been used to characterize observed historical climate and its changes (Alexander et al., 2006). For most statistics the detailed calculation is obvious from the description, though some statistics require additional detail.

Percentile-based threshold levels (statistics 7-10 for temperature in Table 3, and 5-6 for precipitation in Table 4) are calculated for 5-day moving windows through the annual cycle, based on the reference period of 1961-1990. In other words, for each calendar day for the base period, all of the days for each of the 30 years within 2 days of the current calendar day are compiled, and the 10th (or 90th) percentile is determined. Then, for each month and year, the percentage of time that temperature falls below (or exceeds) the historic percentile is calculated. There are two important notes to this technique. First, the daily data are compared relative to varying thresholds throughout the year, and extreme events can be observed with equal probability throughout the year (Klein Tank and Konnen, 2003), so warm periods in the winter are compared to winter 90th percentile

Tmax, for example. Second, as in prior analyses (e.g., Frich et al., 2002), since exceedences would be few in number within any month, monthly values will be less meaningful than annual.

For statistics based on values for multi-day periods (temperature statistics 11 and 15 in Table 3; precipitation statistics 2, 3 and 7 in Table 4), the meaningfulness of these statistics at the monthly level becomes compromised, because the length of the period being assessed (for example, 5 days) becomes large relative to the length of the period being assessed (e.g., a 30-day month). This would cause problems when, for instance, a 5-day dry period spans the 1st of a month, which would then be divided into two shorter dry periods which would not show up as a 5-day dry period. Thus, for these statistics, only annual values are included in our database.

Heating and cooling degree days were calculated using a base temperature of 18 °C (65 °F) following the Encyclopedia of World Climatology (Oliver, 2005). Growing degree days were calculated using a base temperature of 10 °C with no upper threshold used.

Table 3: Temperature-based derivative climate metrics calculated from daily downscaled future climate projections.

<u>Long Name</u>	<u>Variable</u>	<u>Units</u>	<u>Description</u>	<u>Annual</u>	<u>Monthly</u>
Average Low Temperature	tasmin	°C	Monthly mean of daily minimum temperatures		✓
Average High Temperature	tasmax	°C	Monthly mean of daily maximum temperatures		✓
Hottest Temperature	txx	°C	Maximum temperature for the month and year	✓	✓
Coldest Temperature	tnn	°C	Minimum temperature for the month and year	✓	✓
Hot Days Temperature	tx90	°C	Maximum temperatures exceeded the hottest 10% of all days per year	✓	
Number of Frost Days	fd	days	Frost days (min temperature lower than 0°C)	✓	✓
Number of Warm Days	tx90p	%	Very warm days percent: percent of time that daily Tmax values exceed the reference period (1961-1990) 90th percentile Tmax	✓	✓
Number of Cold Days	tx10p	%	Very cold days percent: percent of time that daily Tmax values are below the reference period (1961-1990) 10th percentile Tmax	✓	✓
Number of Warm Nights	tn90p	%	Warm nights percent: percent of time that daily Tmin values exceed the reference period (1961-1990) 90th percentile Tmin	✓	✓
Number of Cold Nights	tn10p	%	Cold nights percent: percent of time that daily Tmin values are below the reference period (1961-1990) 10th percentile Tmin	✓	✓
Heat Wave Duration Index	hwdi	days	Heat wave duration index, number of days per year within intervals of at least 6 days of $T_{max} > (5^{\circ}C + T_{max} \text{ normal for historic period})$. Normal Tmax for historic period is a 5-day running mean	✓	
Growing Degree Days	gd10	days	Growing degree days, for Tavg, sum of degrees > 10°C for each day, but month and year	✓	✓
Heating Degree Days	hd18	days	Heating degree days, calculated with 18°C base temperature, by month and year	✓	✓
Cooling Degree Days	cd18	days	Cooling degree days, calculated with 18°C base temperature, by month and year	✓	✓

Table 4: Precipitation-based derivative climate metrics calculated from daily downscaled future climate projections.

Long Name	Variable	Units	Description	Annual	Monthly
Total Precipitation	pr	mm	Total precipitation for the month and year	✓	✓
Consecutive Dry Days	cdd	days	largest number of consecutive dry days (with daily pr<1mm) per year	✓	
Number of Dry Periods	cdd5	days	number of consecutive dry day periods of length > 5 days, per year	✓	
Number of Wet Days	r02	days	Number of wet days (with precipitation > 0.2mm/day), per month and year	✓	✓
Wet Days	r90p	%	Percent of wet days per year with rainfall> 90-percentile wet-day precipitation, where percentiles are based on ref period 1961-1990. Only days with rainfall>1 mm are considered 'wet'	✓	✓
Wet Day Rainfall	r90ptot	%	Precipitation percent per year due to days with precipitation>90-percentile reference period precipitation	✓	✓
5 Day Rainfall	r5d	mm	Maximum 5-day precipitation total per year	✓	
Daily Rainfall	sdi	mm/day	Simple daily intensity index: the mean daily precipitation on 'wet' days (>1mm)	✓	✓

Derivative Climate Metric Applications

To better understand the utility of these metrics, they have been classified by how they relate to specific real-world applications, such as assessing crop productivity, water supply, flood risk, human health, energy demand, and ecosystem resilience.

Crop productivity relies on many different climate factors including total precipitation, growing degree days, dry days, average low and high temperatures.

Water supply is focused on three precipitation variables: total precipitation—quantifying average water input into the system; and two measures of dryness and drought conditions—consecutive dry days and number of dry periods.

Flood risk is driven by rainfall average, measures of wet day rainfall and short term maximum rainfall intensities.

Human health focuses solely on temperature stress (hot and cold) to people: hottest and coldest single day temperature; number of warm days and cold nights; and the heat wave duration index.

Energy demand incorporates heating and cooling demand using heating and cooling degree days.

Ecosystem resilience to climate change is complex and so incorporates many different aspects including total precipitation, dry conditions, extreme hot and cold temperatures, and growing degree days.

Application	Relevant Derivative Climate Metrics
Crop Productivity	Total Precipitation Consecutive Dry Days Number of Dry Periods Number of Wet Days Growing Degree Days Heat Wave Duration Index Number of Frost Days Hottest Temperature Coldest Temperature Average Low Temperature Average High Temperature
Water Supply	Total Precipitation Consecutive Dry Days Number of Dry Periods
Flood Risk	Total Precipitation Wet Days Wet Day Rainfall 5 Day Rainfall Daily Rainfall
Human Health	Hottest Temperature Coldest Temperature Number of Warm Days Number of Cold Nights Heat Wave Duration Index
Energy Demand	Heating Degree Days Cooling Degree Days
Ecosystem Resilience	Total Precipitation Consecutive Dry Days Number of Dry Periods Average Low Temperature Average High Temperature Hottest Temperature Coldest Temperature Number of Frost Days Growing Degree Days

Quality Control of Derivative Statistics

A comprehensive assessment across all GCMs was conducted to ensure all grid cells in the world fell within expected bounds for all derivative statistics. Appendix 1 shows that all data fall within the expected bounds for all derivative statistics. In addition, the derivative statistics products were spot checked for having values within the range of reasonable values, and were visually checked for any abnormal in spatial patterns. The derivative statistics were inspected for places where NA values should be 0; this occurred with some of the precipitation-based derivative statistics where no precipitation had fallen in a specific month historically.

An evaluation of climate model performance relative to historic observations was conducted for each of the GCMs across the 22 derivative statistics. This analysis was based on the assumption that GCMs that predict historic climate that closely matches historic observations may be more effective at predicting future climate. First, the historic observed derivative statistics were calculated from the historic gridded temperature and precipitation time-series using the same methodology described above. We developed a spatial method using the unpaired Students t-test to quantify the agreement between the GCM modeled historic and observed historic conditions. The computer code was written in the statistical package R.

The analysis was run for all GCM/scenario/model run/derivative statistics combinations, resulting in approximately 3500 maps showing the relative performance of each GCM to match the historic derivative statistic conditions. Values in the maps range from near-zero (historic GCM models significantly deviate from historic observations) to near-one (historic GCM models match historic observations nearly perfectly). These values can be used for weighting future GCM runs based on how well a GCM performed for the past (see section on Climate Model Weighted Ensembles).

Looking across derivative statistics shows that some metrics are better modeled by the GCMs than others when compared with historically observed climate. Table 5 below provides a summary of which climate metrics are modeled better GCM performance on average across all GCMs for each derivative statistic. Statistics with higher values tend to be better represented by the GCMs better (red and orange colors). This measure of climate metric agreement with historic observations can also be mapped out to see where in the world specific derivative statistics perform better or worse.

Table 5: Average historic agreement of GCM with historic observations (p-value) globally among all grid cells (note not area corrected). Higher values indicate better agreement between GCM and historic observations (red = very high agreement; orange = high agreement; yellow = moderate agreement; tan = poor agreement). Note that these p-values are not being used in the traditional sense of finding statistically significant differences between data sets, but rather as a measure of agreement between them—as thus higher values represent higher probability of similarity between the GCMs and observations, whereas lower values lower probability of similarity.

Variable	Ann.	Jan	Feb	Mar	Apr	May	June	July	Aug	Sept	Oct	Nov	Dec
tasmin		0.77	0.77	0.76	0.70	0.68	0.66	0.68	0.65	0.60	0.60	0.59	0.68
tasmax		0.75	0.76	0.74	0.70	0.66	0.66	0.64	0.65	0.61	0.60	0.61	0.66
txx	0.14	0.26	0.26	0.24	0.23	0.19	0.17	0.17	0.18	0.22	0.22	0.23	0.27
tnn	0.20	0.21	0.22	0.21	0.23	0.22	0.20	0.24	0.19	0.20	0.21	0.19	0.18
tx90	0.51												
fd	0.63	0.73	0.56	0.68	0.71	0.65	0.68	0.75	0.68	0.68	0.65	0.70	0.69
tx90p	0.59	0.64	0.64	0.63	0.63	0.63	0.60	0.61	0.61	0.62	0.61	0.63	0.63
tx10p	0.63	0.68	0.69	0.68	0.68	0.68	0.67	0.67	0.66	0.68	0.68	0.68	0.67
tn90p	0.51	0.63	0.63	0.62	0.62	0.61	0.60	0.59	0.59	0.59	0.59	0.60	0.61
tn10p	0.62	0.67	0.70	0.69	0.67	0.68	0.69	0.66	0.68	0.69	0.69	0.69	0.67
hwdi	0.17												
gd10	0.61	0.77	0.69	0.67	0.66	0.52	0.62	0.60	0.60	0.56	0.56	0.67	0.74
hd18	0.63	0.65	0.60	0.65	0.68	0.67	0.68	0.64	0.64	0.62	0.60	0.59	0.62
cd18	0.65	0.83	0.78	0.79	0.71	0.59	0.60	0.63	0.58	0.60	0.66	0.77	0.81
pr	0.80	0.71	0.67	0.69	0.67	0.66	0.65	0.65	0.65	0.64	0.64	0.66	0.68
cdd	0.28												
cdd5	0.26												
r02	0.08	0.35	0.33	0.31	0.26	0.25	0.20	0.19	0.22	0.23	0.29	0.31	0.33
r90p	0.48	0.51	0.51	0.51	0.50	0.50	0.52	0.52	0.50	0.50	0.51	0.52	0.52
r90ptot	0.50	0.55	0.55	0.56	0.56	0.54	0.56	0.55	0.54	0.55	0.55	0.54	0.55
r5d	0.31												
sdii	0.08	0.35	0.35	0.33	0.29	0.29	0.26	0.25	0.24	0.28	0.31	0.32	0.37

Section 4: Climate change analysis and visualization

There are different ways to assess climate change, and a set of climate change statistics is useful. Four statistics for analyzing patterns in climate are: average, departure (or anomaly/difference), p-value, and recurrence interval. The first is a measure of the average climate for the future, and the last three are measures of the amount of change between the past and the future.

Each of the four statistics can be analyzed both spatially at each grid cell, as well as aggregated over a given area of interest (e.g. river basin). This document describes how each of the four statistics is calculated both spatially and aggregated, and how to view and use the results of these calculations as part of the World Bank Climate Wizard Portal

(<http://ClimateKnowledgePortal.ClimateWizard.org>). Below is a description of each type of analysis and maps with examples.

Selection of Time period

The downscaled data in this data set is for a historic baseline time period 1961-1999, for which is calculated for two future time periods: 1) 2046-2065 (most likely estimate for 2055); and 2) 2081-2100 (most likely estimate for 2090). All statistics described use these time periods.

Aggregated versus grid-based analysis

There are two fundamentally different ways to spatially analyze climate change: **aggregated** for an entire area (e.g. country or watershed), and **spatially resolved** across a grid-surface for that area (i.e. grid-based). These two analyses can be useful for different purposes, and should be used in the context of the spatial variation described in the section above.

The aggregated analysis is useful for summarizing climate change over an entire area as a single value. For every area of interest analyzed—e.g. the Nile River Basin—the statistics described above are calculated as averaged over the entire area to give an idea of how the regional area is changing on average. This allows for easier interpretation and for developing climate planning scenarios for that area. Table 6 shows an example from the Nile Basin.

However, solely using aggregated analyses of climate change can be misleading if there are larger regional patterns in climate change. If the area being analyzed is greater than

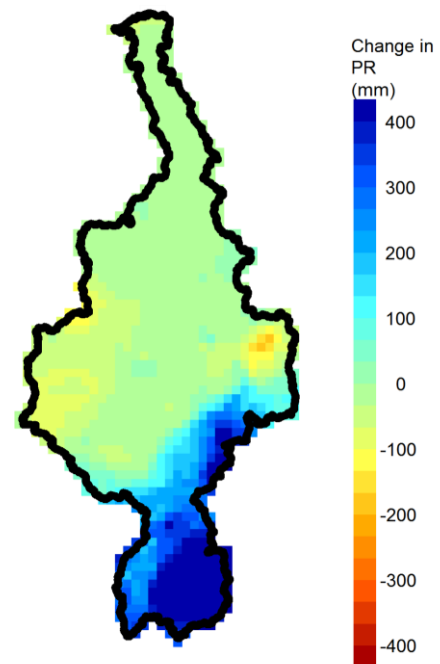


Figure 4: Map of change in annual precipitation by 2081-2100 for the Nile Basin. Blue colors represent increased precipitation, green colors no change, and yellow to red colors decreasing precipitation.

approximately one large climate grid—approximately greater than 100,000 km²—the climate models may show spatial variation of climate change within that area, as they do for change in precipitation the Nile Basin in Figure 4.

Area	Future Time Period	Climate Variable	Model	Emissions Scenario	Month	Past Average (mm)	Future Average	Departure	P-value	Recurrence Interval
Eastern Nile Basin	2081 - 2100	pr	cccma_cgcm3_1.1	a2	14	666	688	22	0.24	2.58
Eastern Nile Basin	2081 - 2100	pr	cnrm_cm3.1	a2	14	678	712	34	0.28	2.82
Eastern Nile Basin	2081 - 2100	pr	gfdl_cm2_0.1	a2	14	654	643	-11	0.63	2.07
Eastern Nile Basin	2081 - 2100	pr	gfdl_cm2_1.1	a2	14	655	779	123	<0.01	6.20
Eastern Nile Basin	2081 - 2100	pr	ipsl_cm4.1	a2	14	690	696	6	0.88	2.58
Eastern Nile Basin	2081 - 2100	pr	miroc3_2_medres.1	a2	14	673	920	247	<0.0001	15.50
Eastern Nile Basin	2081 - 2100	pr	miub_echo_g.1	a2	14	670	864	194	<0.0001	31.00
Eastern Nile Basin	2081 - 2100	pr	mpi_echam5.1	a2	14	673	855	183	<0.0001	31.00
Eastern Nile Basin	2081 - 2100	pr	mri_cgcm2_3_2a.1	a2	14	671	735	64	<0.0001	3.10
Eastern Nile Basin	2081 - 2100	pr	Ensemble average	a2	14	670	766	96		10.76

Table 6: This table shows the average non-spatial values averaged over the entire Eastern Nile River Basin between the periods 1961-1990 and 2081-2100. The *Departure* value represents the difference between the aggregate means: *Past Average* and *Future Average*. The p-value give the statistical confidence in the future change (p<0.05 is a significant change), and the recurrence interval relates the future average condition to the frequency of climate extremes in the past (e.g. what happened once every 10 years in the past is projected to every other year in the future).

Different Types of Climate Change Analyses

Summary of different types of climate analysis measurements

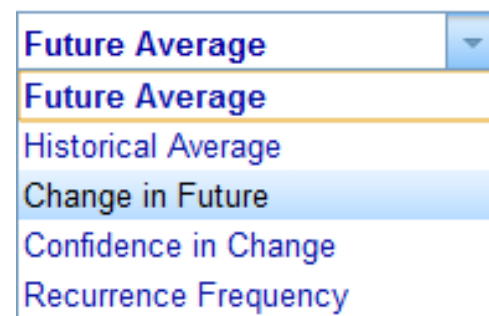
Average: average climate value during future time period (does not represent change)

Departure: amount of change between historic baseline average climate value and future average climate value

p-value: Statistical significance of change between baseline average climate value and future average climate value

Recurrence Interval: How much more often extreme events will occur in the future than occurred in the past.

Measurement



Each of the four statistics can be viewed as interactive maps (spatial) in the primary CWC interface. To switch between each statistic, click on one of the four radio buttons under *Map Options* on the left panel of the Climate Wizard interface:

Any map being viewed can be downloaded in GIS format or as a graphical map image from the links under “Downloads”.

Average climate

The mean of each climate variable is calculated across either monthly or annual time *domains* (user-specified) and across one of two user-specified future time *periods* (2046-2065 or 2081-2100).

Mean calculations are only performed within user-specified polygon boundaries (heretofore referred to as the “area”). The calculation can be expressed as:

$$\text{Spatial equation (map)} \quad \bar{x}_i = \{mean(x)\}_{T,i}$$

$$\text{Non-spatial equation (table)} \quad \bar{x} = mean(\bar{x}_i)$$

where \bar{x}_i and \bar{x} (spatial and non-spatial means) are summarized across the time domain set, T , and pixel set, i . The non-spatial mean aggregates all pixels within the user-specific area, and therefore describes the area as a whole.

A spatially resolved example is provided for the hottest day of the year across Africa and the Middle East comparing the average for 1961-1990 to the average for 2081-2100 (Figure 5). Note how much hotter the hottest day of the year is projected to be by 2081-2100.

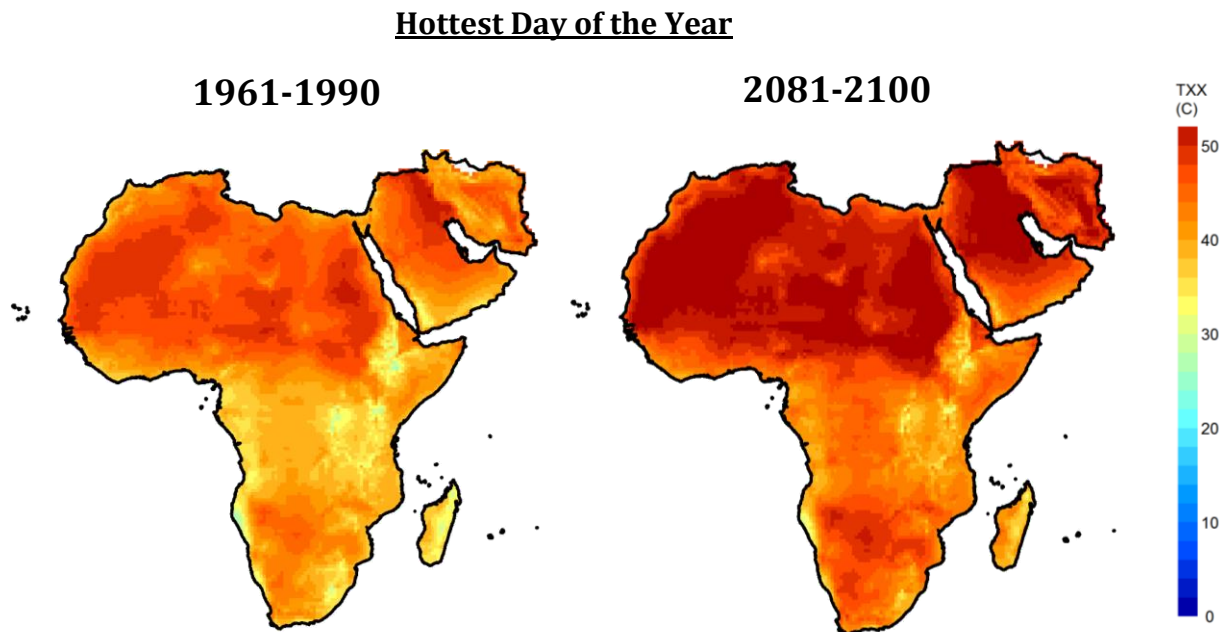


Figure 5: Projected average annual consecutive dry days in the Africa and Middle East World Bank regions for the period 1961-1990 (historic baseline emissions) and 2081-2100 (A2 emissions). The color of each pixel represents the total annual precipitation averaged over the entire time period.

Departure change analysis

The departure (or difference) of each climate variable is calculated as the difference between future and historic periods. The historic period is always 1961-1990 and the future period can be defined as either 2046-2065 or 2081-2100.

Spatial equation (map):

$$\delta_i = \bar{x}_{i,F} - \bar{x}_{i,P}$$

Non-spatial equation (table):

$$\delta = \bar{x}_F - \bar{x}_P$$

where δ_i and δ (spatial and non-spatial departures) are simply the differences of the future and past means, \bar{x}_F and \bar{x}_P respectively. The spatial departure, δ_i , is calculated at every pixel, i , and the non-spatial departure, δ , is calculated from the past and future means in the summary table.

A spatial example (from Climate Wizard Website, <http://ClimateWizardCustom.org/extremes>) for change in Consecutive Dry Days in 2081-2100 for the Africa region (Figure 6) and change in precipitation for the Nile River Basin (Figure 4)

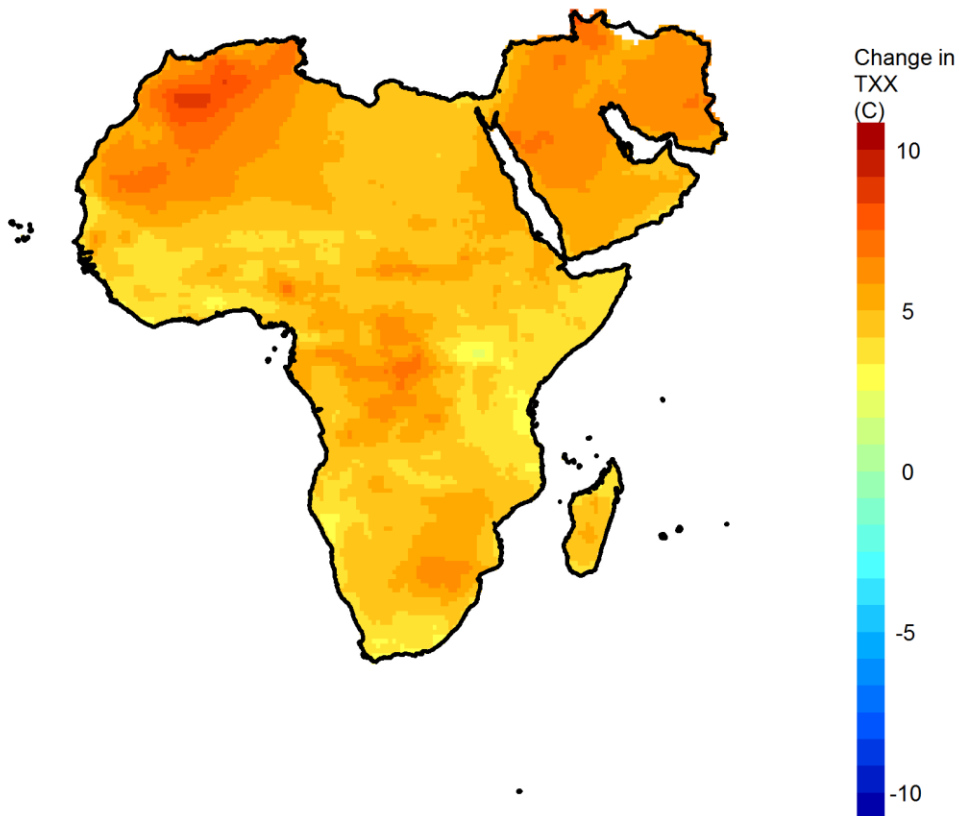


Figure 6: Map of change in annual maximum temperature for the GFDL_cm2_0.1 climate model A2 emissions scenario for 2081-2100.

P-value: statistical confidence in change

The p-value describes the probability that the future projections are different than the past using Student's t-test. Classical statistics generally interprets p-values of 0.10, 0.05, and 0.01 to be “marginally significant,” “significant,” and “highly significant,” respectively. A “significant” p-value means that there is 95% $([1 - 0.05] * 100\%)$ certainty that the shift in the data did not occur at random. Therefore, the lowest p-values in the maps and tables can be interpreted as the strongest shifts in pattern from the historic climate to the projected future. The p-values in the maps and tables do NOT describe the certainty that the future climate will actually occur, as different models could project different degrees of change. Additionally, the Student's t-test assumes that the distributions of the future and past sets are normal, which may not be the case depending on the climate variable (Figure 7).

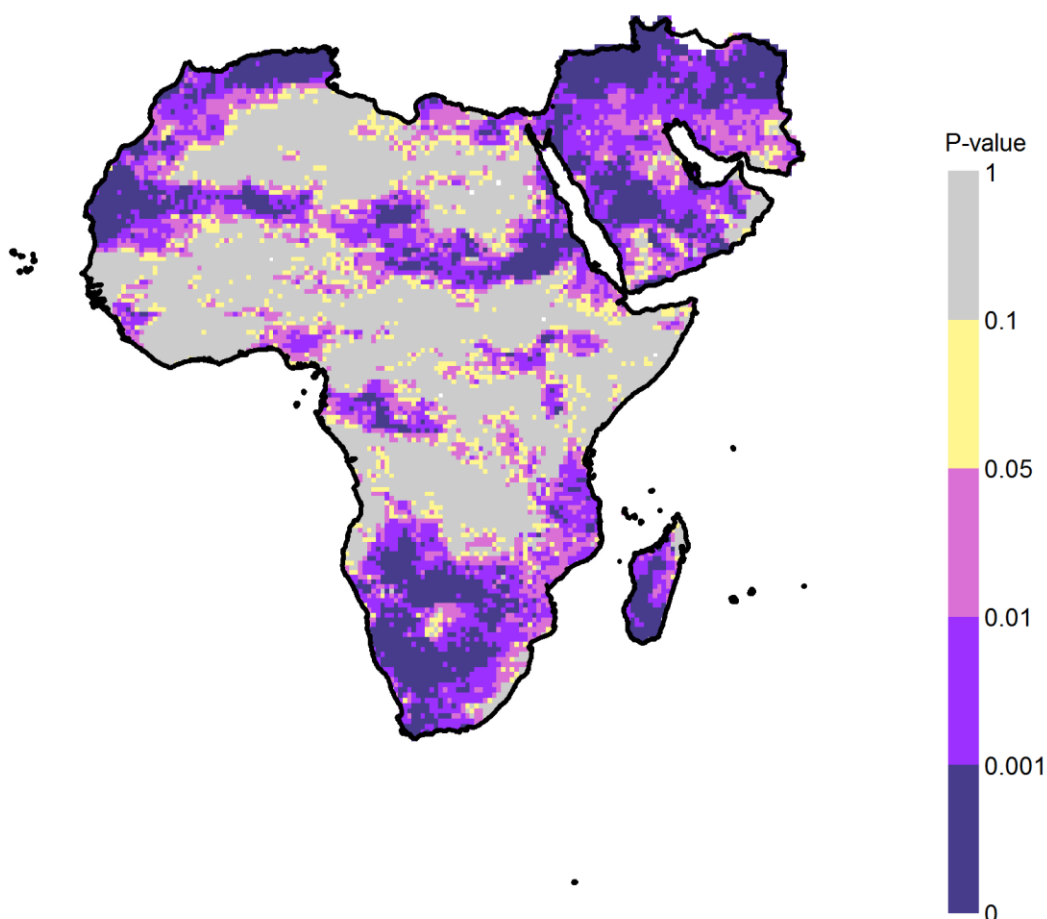


Figure 7: The probability (p-value) that the difference between past and future annual precipitation is not random. Grey pixel values between 0.1 and 1 describe an “insignificant” change from past to future that could have occurred at random. Conversely, dark purple pixel values between 0 and 0.001 describe a “highly significant” change from past to future that has less than a 0.1% chance of occurring at random.

Future recurrence interval

The recurrence interval statistic describes how often the future median climate variable would have been expected to happen in the past. In other words, answering the question “In our recent historic climate (e.g. 1961-1990), how often did we experience events that we expect to be commonplace in the future”. For example, a recurrence interval value of 10 means that events that we only saw once every 10 years during the recent past (1961-1990) will be expected to happen every other year in the future.

Spatial equation (for creating map):

$$fpo_i = \frac{\{rank(\tilde{x}_{i,f})\}_{i,p}}{N_p + 1}$$

$$fri_i = \begin{cases} fpo_i \geq 0.5; 1/1 - fpo_i \\ fpo_i < 0.5; 1/fpo_i \end{cases}$$

Non-spatial equation (for creating table):

$$fpo = \frac{\{rank(\tilde{x}_f)\}_p}{N_p + 1}$$

$$fri = \begin{cases} fpo \geq 0.5; 1/1 - fpo \\ fpo < 0.5; 1/fpo \end{cases}$$

where fpo is the future probability of occurrence; $\tilde{x}_{i,f}$ is the median of the future set at each pixel, i ; p is the past set; N_p is the sample size of the past set; and fri is the future recurrence interval. The non-spatial recurrence interval is calculated like the recurrence interval at each pixel in the spatial calculation, except that the climate variable is spatially averaged (\tilde{x}_f) before finding the median across the future set (\tilde{x}_f). The maximum recurrence interval possible is 31 because there are only 30 years in the past set. If $\tilde{x}_{i,f}$ or \tilde{x}_f are outside the range of values of the past set, a value of 100 is assigned. The value of 100 is arbitrary. It denotes a scenario where the median future event was not experienced within the 30-year historic period (i.e., a “novel” climate, Figure 8).

Recc. int. of Annual Consecutive Dry Days
gfdl_cm2_0.1 A2 2081 - 2100

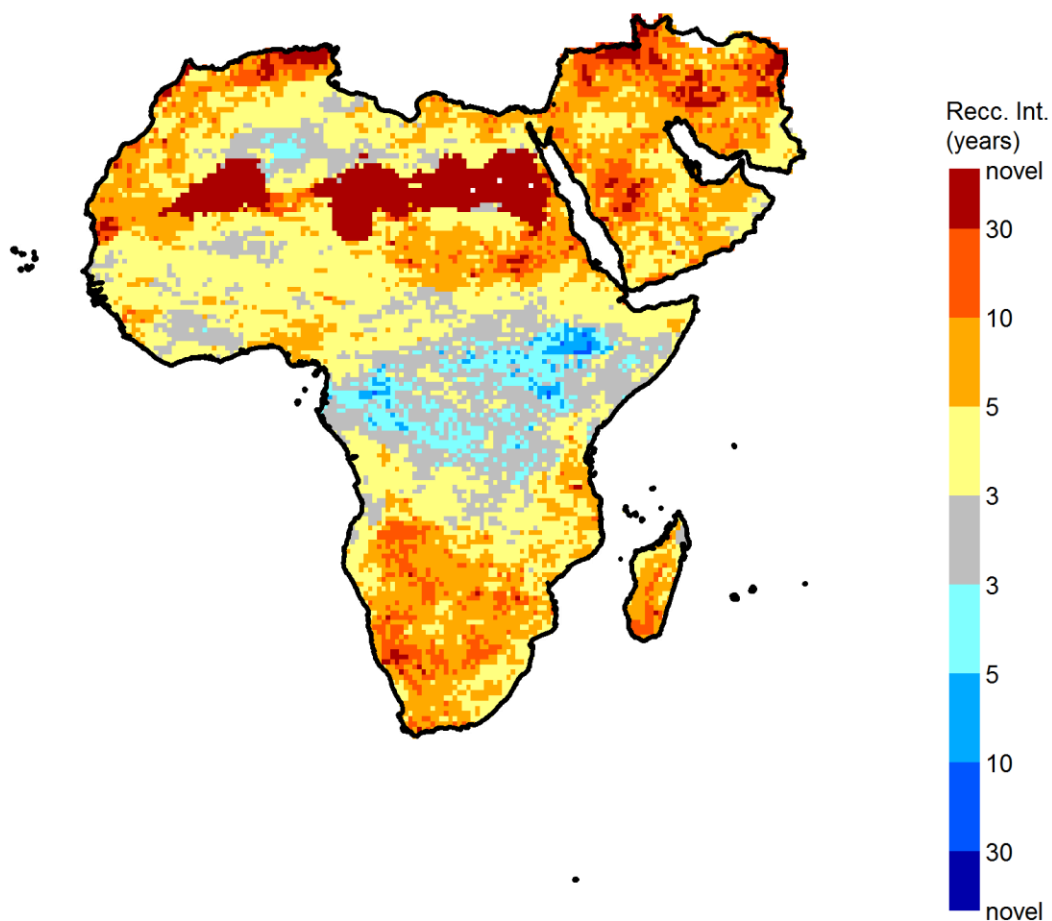


Figure 8: shows the average change in recurrence interval of the 2081-2100 median model for consecutive dry days: what historically occur once every 3-10 years during 1961-1990, is projected to occur every other year in the future. Blue pixels denote increased occurrence of high precipitation events (i.e. future precipitation is greater in the future than the past precipitation) and yellow-red pixels denote recurrence intervals of low precipitation events (i.e. the future precipitation is less than the past median). The darkest hues of blue or red describe future scenarios where the average year is future year is projected to experience fewer levels that never occurred during 1961-1990.

Ensemble Analysis

Climate change analysis becomes more complex for the future than the past because there is not one time-series of climate, but rather many future projections from different GCMs run with a range of CO₂ emissions scenarios (IPCC 2007b). It is important not to analyze only one GCM for any given emission scenario, but rather to use ensemble analysis to combine the analyses of multiple GCMs and quantify the range of possibilities for future climates under different emissions scenarios. There are many approaches for doing ensemble analysis ranging from simple averaging approaches to more complex and computationally intensive probability estimation approaches (Dettinger 2006, Araujo and New 2007).

Quantile ensembles

The multiple climate model maps are combined together using a simple, yet informative non-parametric quantile-rank approach that maps out the 0 (minimum), 20, 40, 50 (median), 60, 80, and 100th (maximum) percentiles. The range of a climate variable across the different ensembles shows you the range in the climate models for that variable.

Ensembles can be interpreted differently for temperature versus precipitation. For temperature, all models agree that mean temperatures will increase everywhere in the world, so the ensemble shows you different magnitudes of temperature increase. However for precipitation, all models often do not agree on the direction of change, much less the magnitude in either direction. Ensemble analysis can be used to understand the distribution of climate models, look for climate model agreement, and identify the range of future climate projections. A spatially-resolved example of an ensemble analysis is given for change in consecutive dry days by 2081-2100 under the A2 emissions scenario (Figure 9 left)

Climate model-weighted ensembles

Ensembles of climate models weighted to incorporate information about how well each GCM related to the represented observed climate. For each climate variable, each climate model was compared to historic observations of climate to determine how well they matched in each grid cell globally. Then the climate models were averaged weighted by how well the model matched the historic observations. A spatially-resolved example of an ensemble analysis is given for change in consecutive dry days by 2081-2100 under the A2 emissions scenario (Figure 9 right). Note that there is not much difference between using the weighted ensemble as compared to the un-weighted ensemble (Figure 9).

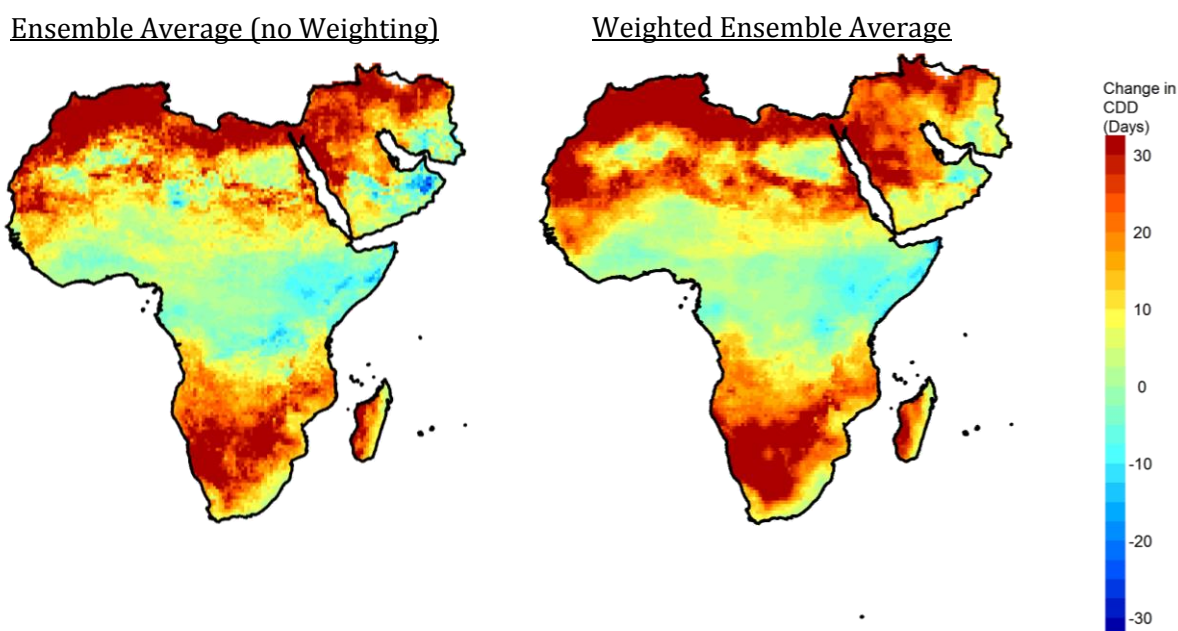


Figure 9: Maps of ensemble average unweighted median of climate models and weighted ensemble average (weighted mean) for change in consecutive dry days in 2081-2100 (A2 Emission scenario). Note a great similarity among the patterns of change between the two methods for calculating ensemble.

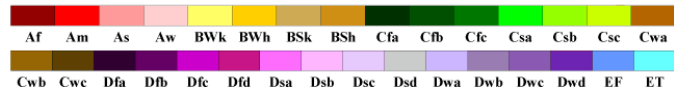
Looking at regional patterns versus single climate grid cell

Assessing regional patterns in climate change is important for understanding if climate change is consistent for the area or if climate change varies regionally. Often climate change will have different patterns for different. For example, change in consecutive dry days over the Africa and Middle World Bank regions varies from large increases in the northern and southern parts to large decreases in Central and Sub-Saharan regions (see Figure 9). However, for analyses of smaller areas—such as the country of Mali in west Africa—the results will be much more spatially consistent (increasing number of consecutive dry days).

These regional patterns can be analyzed in relation to the Koeppen Climate Zones (Figure 10) which classify the world by arid to moist regions, precipitation seasonality, and different temperature ranges. Looking at the change in consecutive dry days relative to the Koeppen regions shows similar spatial patterns between the zones and climate change (Figures 10 & 11). This shows that if the area you are analyze spans different climate regions, it is even more important to assess the spatial variation in climate change.

World Map of Köppen–Geiger Climate Classification

updated with CRU TS 2.1 temperature and VASCLimO v1.1 precipitation data 1951 to 2000



Main climates

- A: equatorial
- B: arid
- C: warm temperate
- D: snow
- E: polar

Precipitation

- W: desert
- S: steppe
- f: fully humid
- s: summer dry
- w: winter dry
- m: monsoonal

Temperature

- h: hot arid
- k: cold arid
- a: hot summer
- b: warm summer
- c: cool summer
- d: extremely continental
- F: polar frost
- T: polar tundra

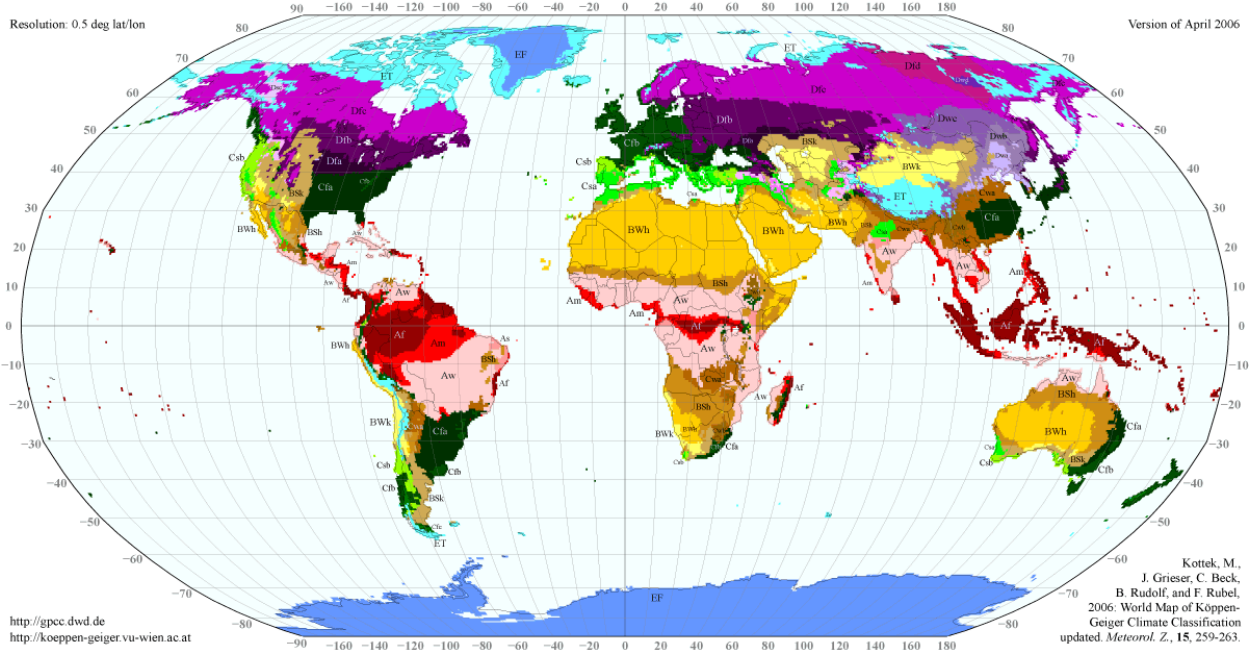


Figure 10: Koeppen’s Climate Classification (obtained from: <http://koeppen-geiger.vu-wien.ac.at/present.htm>)

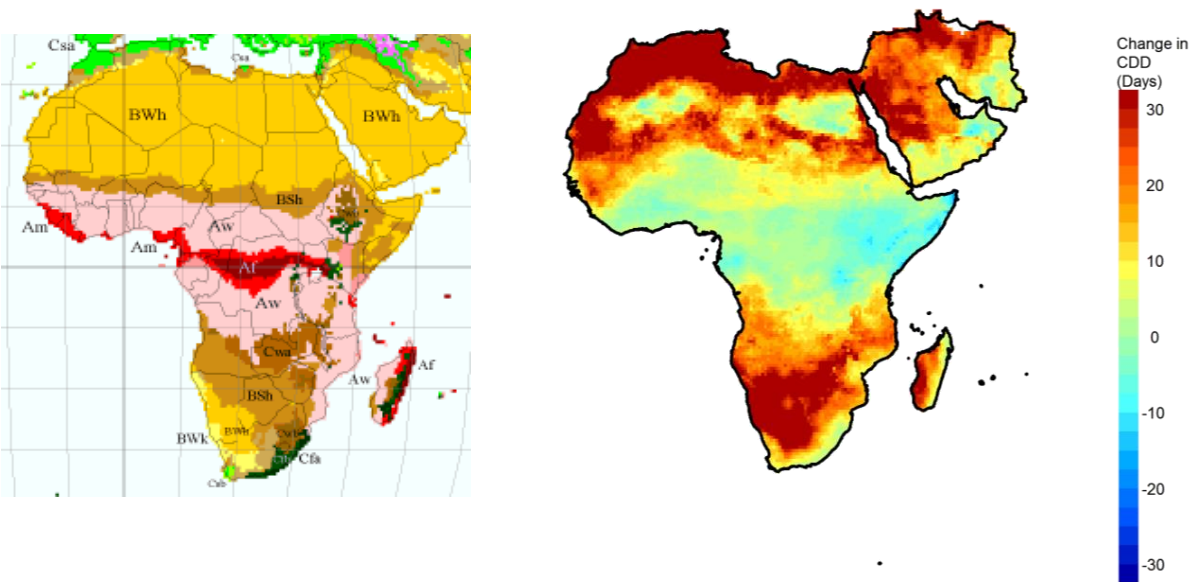


Figure 11: Notice the spatial relationship between change in consecutive dry days and the Koeppen climate regions for Africa and Middle East (See figure 10 for Koeppen Region descriptions).

Section 5: Using daily downscaled data in impact modeling

Collaboration with Dr. Jawoo Koo (International Food Policy Research Institute), Dr. Zhiming Qi (International Food Policy Research Institute), and Dr. Jorge Escurra (World Bank)

Downscaled climate data at the daily time scale is very important for impact modeling—especially for water resources, agriculture, among others—and the data described in this document here can be directly used in agricultural crop models and hydrological water resources models. Two case studies were conducted to demonstrate the utility of daily downscaled data: 1) hydrologic impacts of climate change in the Nile Basin using SWAT modeling; 2) food security impacts in Egypt and Ethiopia using the DSSAT crop model (in collaboration with the International Food Policy Research Institute).

The first case study demonstrates how daily downscaled climate data can be useful for calibrating a hydrological model (Figure 12). Since the daily variation comes from the climate model, they have spatial correlation in weather events (i.e. when a large storm comes through many neighboring grid cells have precipitation at the same time), and temporal correlation (i.e. the rain may last for multiple days in the grid cells). These correlations are important for more accurately modeling river flows.

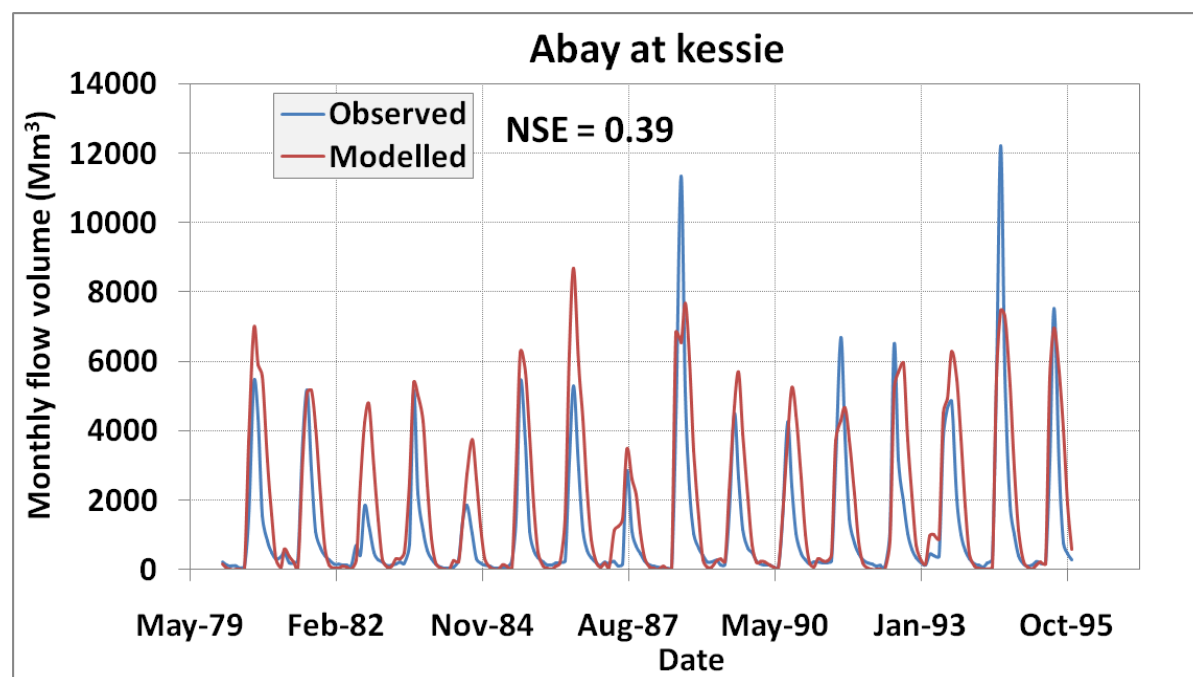


Figure 12: Historic observed and modeled from gridded climate data for flow stations (a) Blue Nile at Khartoum and (b) Abay at Kessie.

The second case study shows the utility of these daily downscaled climate data for crop modeling. It successfully modeled crop yields in Egypt and Kenya. For one, this case study shows that the daily downscaled climate model data simulated greater the year-to-year variation in crop yields than did the weather generator. This is important as it is especially the low yield years that are most important for food security issues (Figure 13).

Second this case study shows that the use of fertilizer and irrigation can be optimized to produce the greatest increase in yield per unit of application, which is important for adaptation planning. It shows that there is a positive and increasing return on application of both irrigation and Nitrogen fertilizer up to a certain point, then there is virtually no return on application (Figure 14 and 15a). In addition, this shows that with climate change the optimal application of irrigation will change with future climate, and that 13% more irrigation will be required to obtain the optimum yield, and that even with the increase in irrigation the maximum yield will be reduced by 30% compared to the historic climate. This provides information to agricultural managers to know under which circumstances crop yields can be most improved in the face of climate change.

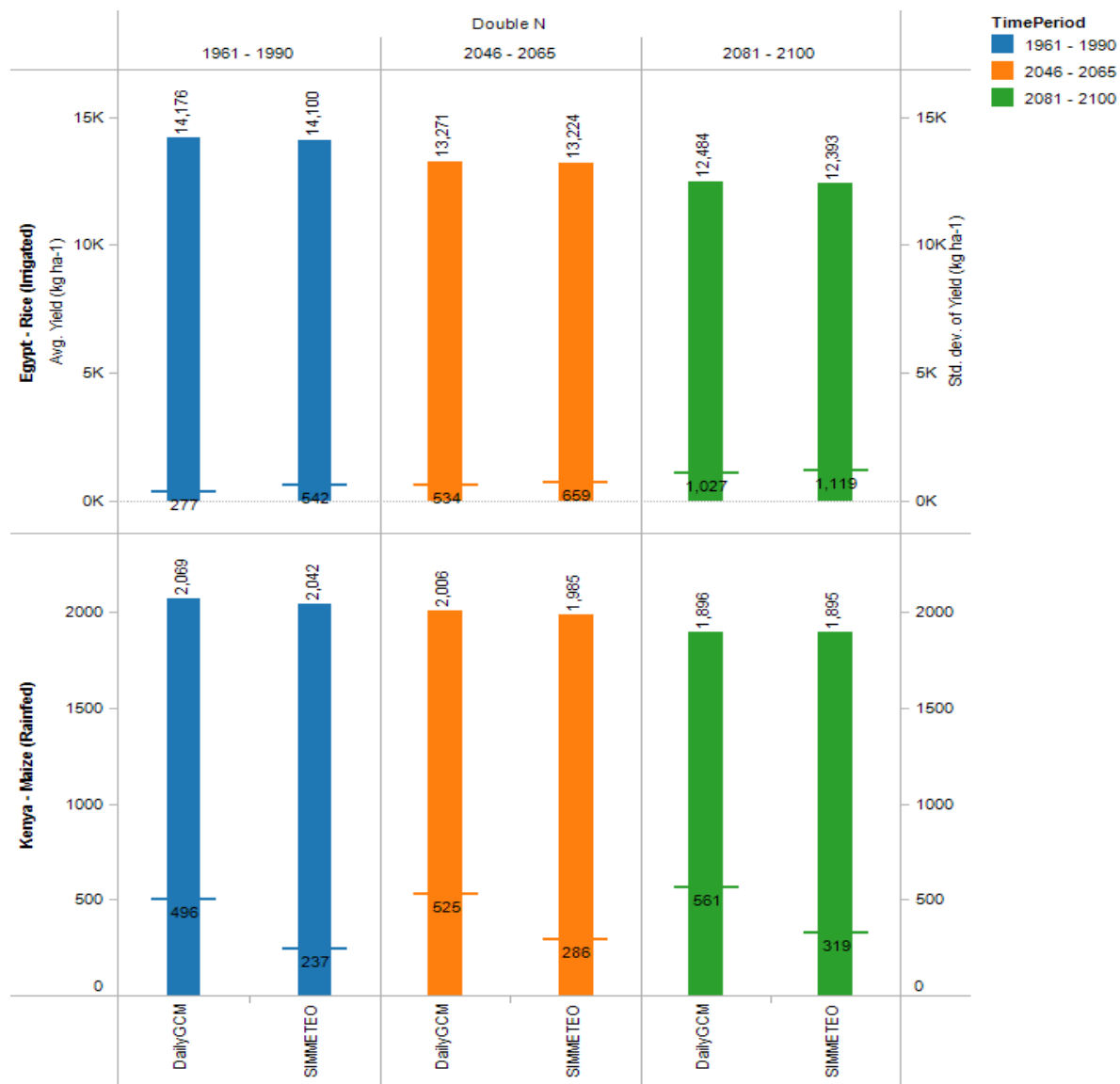


Figure 13: DSSAT modeled crop yields with double Nitrogen using the daily downscaled future climate projections from Girvetz et al. 2012 compared to DSSAT modeled crop yields based on weather generator data. Note that the average yields are very similar, but the variance in yields represented by the horizontal lines is decreased when the weather generator data is used.

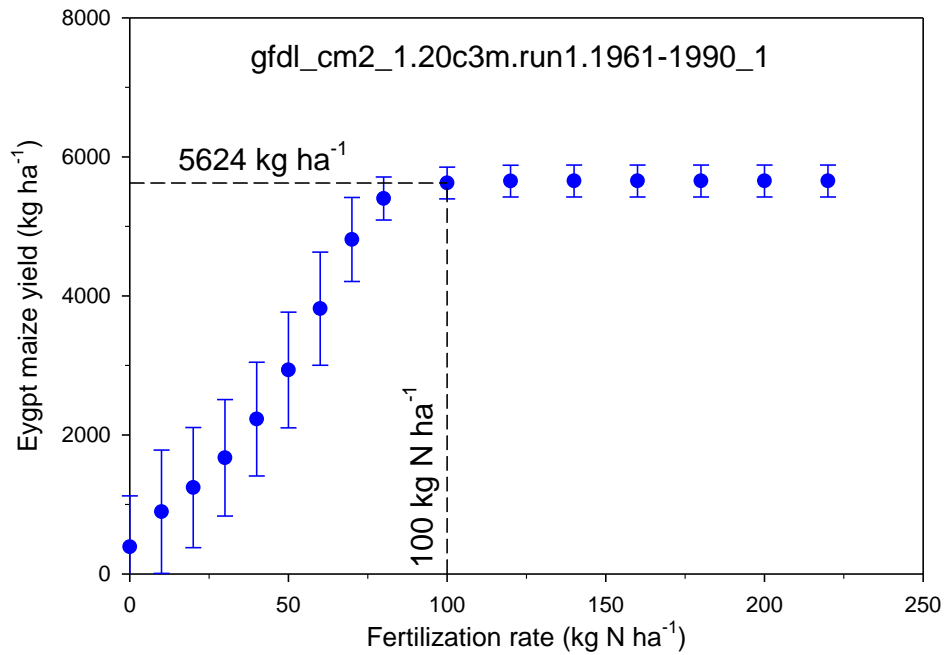


Figure 14: Maize yield response to fertilization rate at a site in Egypt. Note that fertilization above approximately 100 kg N ha⁻¹ does not improve yields, but that increasing N application between 50-100 kg N ha⁻¹ marginally improved yields more than increasing N application between 0-50.

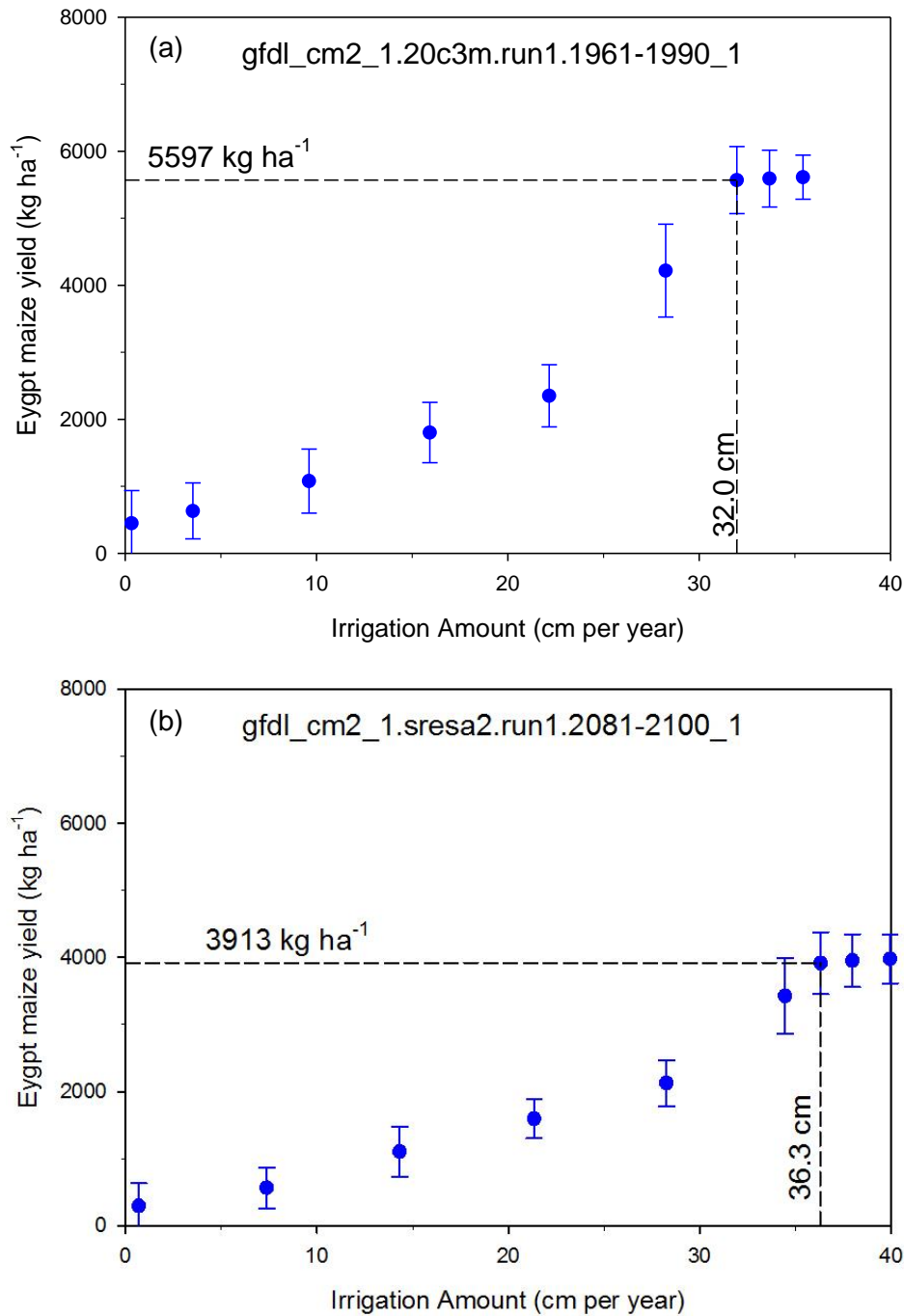


Figure 15: Maize yield to irrigation at an Egypt site as simulated by RZWQM2 model in the (a) historic climate 1961-1990, and (b) in the future climate 2081-2100. Note the optimal irrigation rate increases in the future by 13.4 % (from 32.0 to 36.3 cm), and even with this increase in irrigation the overall yield is reduced in the future by 30% (from 5597 to 3913 kg/ha).

Cited References

- Abatzoglou, J. T. and Brown, T. J. (2011), A comparison of statistical downscaling methods suited for wildfire applications. *International Journal of Climatology*, 31: n/a. doi: 10.1002/joc.2312
- Alexander, L. V., et al. , 2006. Global observed changes in daily climate extremes of temperature and precipitation, *J. Geophys. Res.*, 111(D5), D05109.
- Barnett, T. P., Pierce, D. W., Hidalgo, H. G., Bonfils, C., Santer, B. D., Das, T., Bala, G., Wood, A. W., Nozawa, T., Mirin, A. A., Cayan, D. R., and Dettinger, M. D.: Human-Induced Changes in the Hydrology of the Western United States, *Science*, 319, 1080-1083, doi:10.1126/science.1152538, 10.1126/science.1152538, 2008.
- Beyene, T., Lettenmaier, D., and Kabat, P.: Hydrologic impacts of climate change on the Nile River Basin: implications of the 2007 IPCC scenarios, *Climatic Change*, 100, 433-461, 10.1007/s10584-009-9693-0, 2010.
- Cayan, D., Luers, A., Franco, G., Hanemann, M., Croes, B., and Vine, E.: Overview of the California climate change scenarios project, *Climatic Change*, 87, 1-6, 10.1007/s10584-007-9352-2, 2008.
- Easterling, D. R., L. V. Alexander, A. Mokssit, and V. Detemmerman, 2003. CCI/CLIVAR Workshop to Develop Priority Climate Indices, *Bull. Am. Met. Soc.*, 84(10), 1403-1407.
- Frich, P., L. V. Alexander, P. Della-Marta, B. Gleason, M. Haylock, A. M. G. Klein Tank and T. C. Peterson, 2002. Observed Coherent changes in climatic extremes during the second half of the twentieth century. *Clim. Res.* 19:193-212.
- Hayhoe, K., Wake, C., Anderson, B., Liang, X.-Z., Maurer, E., Zhu, J., Bradbury, J., DeGaetano, A., Stoner, A., and Wuebbles, D.: Regional climate change projections for the Northeast USA, *Mitigation and Adaptation Strategies for Global Change*, 13, 425-436, 10.1007/s11027-007-9133-2, 2008.
- Hayhoe, K., Cayan, D., Field, C. B., Frumhoff, P. C., Maurer, E. P., Miller, N. L., Moser, S. C., Schneider, S. H., Cahill, K. N., Cleland, E. E., Dale, L., Drapek, R., Hanemann, R. M., Kalkstein, L. S., Lenihan, J., Lunch, C. K., Neilson, R. P., Sheridan, S. C., and Verville, J. H.: Emissions pathways, climate change, and impacts on California, *Proc. National Academy Sci.*, 101, 12422-12427, 2004.
- Karl, T. R., N. Nicholls, and A. Ghazi, 1999. Clivar/GCOS/WMO Workshop on Indices and Indicators for Climate Extremes Workshop Summary, *Climatic Change*, 42(1), 3-7.
- Klein Tank, A. M. G. and G. P. Können, 2003. Trends in Indices of Daily Temperature and Precipitation Extremes in Europe, 1946–99. *J. Climate* 16:3665-3680.

Maraun, D.: Nonstationarities of regional climate model biases in European seasonal mean temperature and precipitation sums, *Geophys. Res. Lett.*, 39, L06706, 10.1029/2012gl051210, 2012.

Maurer, E. P., J. C. Adam, and A. W. Wood, 2009. Climate model based consensus on the hydrologic impacts of climate change to the Rio Lempa basin of Central America. *Hydrology and Earth System Sciences* 13:183-194.

Maurer, E.P. and H.G. Hidalgo, 2008. Utility of daily vs. monthly large-scale climate data: an intercomparison of two statistical downscaling methods, *Hydrology and Earth System Sciences* Vol. 12, 551-563. ([HESS On-line Paper](#))

Oliver, J. E, 2005. *Encyclopedia of World Climatology*. Springer. The Netherlands. 854 pp.

Schulzweida, U., L. Kornblueh, and R. Quast, 2011. CDO User's Guide, Climate Data Operators, Version 1.5.0, MPI for Meteorology, March 2011, 183 pp.

von Engelen, A., A. Klein Tank, G. ven de Schrier, and L. Klok, 2008. Towards an operational system for assessing observed changes in climate extremes: European Climate Assessment & Dataset (ECA&D)Rep., 40 pp, KNMI, The Netherlands.

Wood, A. W., Maurer, E. P., Kumar, A., and Lettenmaier, D. P.: 2002. Long Range Experimental Hydrologic Forecasting for the Eastern U.S. *Journal of Geophysical Research* 107 (D20), 4429.

Wood, AW, LR Leung, VR Sidhar, and DP Lettenmeier. 2004. Hydrologic Implications of Dynamical and Statistical Approaches to Downscaling Climate Model Outputs. *Climatic Change* 62: 189-216.

Appendix 1: Quality control for daily downscaled climate models

For precipitation results, we checked for

1. Negative values of precipitation.
2. Daily precipitation values in excess of 400 mm/day. Such values are not necessarily erroneous, but they should not occur too often. We calculated the rate of occurrence of such values in the 20th and 21st centuries.
3. Locations where precipitation occurs every day.

The following Tables A1.1 show the results of this quality control analysis:

Model Name	20C	B1	A1B	A2
CGCM3.1 (T47)	641	862	1274	1371
CNRM-CM3	604	558	1068	1438
GFDL-CM2.0	447	1022	1106	1084
GFDL-CM2.1	530	886	1431	1469
IPSL-CM4	573	822	862	1052
MIROC3.2 (medres)	605	574	947	681
ECHO-G	636	881	1330	1106
ECHAM5/ MPI-OM	568	682	N/A	820
MRI-CGCM2.3.2	521	556	819	686

Table A1.1: Number of grid cells with precipitation values in excess of 400 mm/day. Note this is out of approximately 4.5 billion bias corrected and statistically downscaled grid cells, showing these occur approximately 1 in every 5,000,000 grid cells. It is expected that some grid cells will be greater than 400 mm precipitation for specific days.

For daily minimum and maximum temperatures, the following were checked:

1. The maximum value of Tmax and the minimum value of Tmin for both the 20th and 21st century periods (see table below for minimum and maximum values for both Tmin and Tmax).
2. The number of cases where Tmin < -50 C, and Tmax > 50 C
3. Compared at each location the median values of bias-corrected (but not downscaled) model results to those in observations. By design, the median value for the bias-corrected data (for the 30-day moving window) should precisely agree with the 30-day moving window median value of the observed data.

4. Compared at each location the overall trend before vs. after bias correction. The bias correction procedure is designed to preserve trends.

The following tables A1.2-A1.4 show the results of this quality control analysis:

Model Name	20C	B1	A1B	A2
CGCM3.1 (T47)	-91.83	-81.37	-80.71	-82.94
CNRM-CM3	-89.06	-89.90	-80.80	-86.64
GFDL-CM2.0	-87.86	-83.89	-84.64	-86.44
GFDL-CM2.1	-89.98	-81.96	-81.87	-85.04
IPSL-CM4	-91.80	-80.57	-79.82	-82.68
MIROC3.2 (medres)	-86.24	-77.30	-76.84	-81.31
ECHO-G	-90.90	-81.81	-85.55	-82.37
ECHAM5/ MPI-OM	-87.17	-81.60	N/A	-81.00
MRI-CGCM2.3.2	-91.75	-85.50	-82.27	-87.73

Table A1.2: Minimum values for Tmin among all grid cells:

Model Name	20C	B1	A1B	A2
CGCM3.1 (T47)	42.40	44.09	47.15	47.14
CNRM-CM3	42.69	44.39	46.30	48.76
GFDL-CM2.0	42.22	45.66	48.51	48.32
GFDL-CM2.1	42.40	44.96	47.89	48.20
IPSL-CM4	42.31	45.38	47.67	46.60
MIROC3.2 (medres)	43.18	45.99	48.02	48.91
ECHO-G	42.40	45.62	48.15	48.29
ECHAM5/ MPI-OM	42.20	47.57	N/A	48.30
MRI-CGCM2.3.2	42.29	44.56	45.39	47.97

Table A1.3: Maximum values for Tmin among all grid cells:

Model Name	20C	B1	A1B	A2
CGCM3.1 (T47)	-74.04	-65.41	-66.41	-63.74
CNRM-CM3	-74.03	-69.27	-63.66	-64.49
GFDL-CM2.0	-70.00	-67.07	-68.81	-68.14
GFDL-CM2.1	-74.07	-66.71	-64.31	-64.30
IPSL-CM4	-69.96	-64.52	-63.52	-70.62
MIROC3.2 (medres)	-69.78	-64.60	-63.67	-64.91
ECHO-G	-73.91	-66.18	-63.55	-63.27
ECHAM5/ MPI-OM	-74.06	-66.88	N/A	-65.55

MRI-CGCM2.3.2	-69.22	-66.36	-66.77	-65.14
---------------	--------	--------	--------	--------

Table A1.4: Minimum values for Tmax among all grid cells:

Model Name	20C	B1	A1B	A2
CGCM3.1 (T47)	61.88	61.56	62.51	61.95
CNRM-CM3	60.36	65.24	65.20	64.47
GFDL-CM2.0	62.54	62.18	64.94	66.18
GFDL-CM2.1	63.67	65.87	64.52	67.03
IPSL-CM4	62.08	64.45	64.22	66.29
MIROC3.2 (medres)	60.54	63.26	64.02	66.55
ECHO-G	62.03	61.55	64.93	64.46
ECHAM5/ MPI-OM	61.34	63.93	N/A	65.84
MRI-CGCM2.3.2	60.89	62.09	63.02	64.97

Table A1.5: Maximum values for Tmax among all grid cells:

Appendix 2: Derivative statistics data ranges for summarized across all climate models

These were calculated across all grid cells in the world, GCMs, model runs, emissions scenarios, and time periods. The minimum and maximum were calculated both across all years (i.e. the highest single year) and for the averages of the three time periods (1961-1999, 2046-2065, 2081-2099). Note that rounding can cause values to be outside of the expected range by < 1% (e.g., TN90P, TX90P).

Variable	Annual					Monthly				
	Minimum All Years	Minimum 20/38 yr Normal	Mean	Maximum 20/30 yr normal	Maximum All Years	Minimum All Years	Minimum 20/30 yr Normal	Mean	Maximum 20/30 yr normal	Maximum All Years
CD18	0	0	1,363	6,559	7,209	0	0	114	547	896
CDD	0	6	64	365	366					
CDD5	0	1	12	22	31					
FD	0	0	117	365	366	0	0	10	30	31
GD10	0	0	2,868	9,479	10,129	0	0	239	790	1,144
HD18	0	0	3,931	16,721	18,811	0	0	328	1,393	2,500
HWDI	0	0	55	330	364					
pr	0	0	824	16,944	24,040	0	0	69	1,412	11,067
R02	0	0	135	348	365	0	0	11	29	31
R5D	0	0	42	791	1,429					
R90P	0	0	13	46	100	0	0	11	32	100
R90PTOT	0	0	37	81	100	0	0	24	61	100
SDII	1	1	8	103	175	1	1	7	78	695
tasmax	-48	-21	17	42	45	-59	-20	17	43	55
tasmin	-65	-40	5	31	33	-75	-39	5	31	42
TN10P	0	1	3	25	98	0	1	3	24	100
TN90P	0	11	37	101	101	0	11	37	100	100
TNN	-90	-69	-16	26	28	-90	-48	-2	28	40
TX10P	0	1	4	28	99	0	1	4	28	100
TX90	-9	-4	29	53	54					
TX90P	0	11	33	100	101	0	11	33	100	100
TXX	-6	1	35	57	65	-51	-13	23	47	65